## *The polarisation of the cone(IRN) Nebula in NGC 2264*

Marianne C.M. Hill

# THE POLARISATION OF THE CONE(IRN) NEBULA IN NGC 2264

MARIANNE C. M. HILL

A Thesis submitted to the University of Durham for the degree of Master of Science.



Department of Physics.
September 1991

The copyright of this thesis rests with the author. No quotation from it should be published without his prior written consent and information derived from it should be acknowledged.

# ABSTRACT.

The first part of this thesis presents a general review of interstellar gas and dust, and how the study of nebulae has developed. The property of the linear polarisation of light from astronomical objects is a mechanism which has enabled astronomers to extend their knowledge and understanding considerably. Polarisation studies of nebulae have given information on nebular structures, grain size and composition, and the geometrical structures involved. The methods of producing polarisation are discussed, and various models proposed which explain the various observed features.

The second part of the thesis deals specifically with the Cone(IRN), which is a small "fan" shaped nebula, found within NGC 2264, very near to Allen's Infrared object (GL989). Chapter four presents a review of the current knowledge of NGC 2264, and research conducted by other astronomers on the cone(IRN). It explains why it is of particular interest and relevant to this thesis, and also includes some interpretations as to the mechanisms contributing to the observed polarisation. This then leads into the polarisation data, including a brief outline of the construction of the polarimeter. The polarisation maps are presented in the V,R,I filters, and the wavelength dependence of the polarisation is calculated.

Chapter six discusses the data, and the possible mechanisms involved. From the results, it is clear that the Cone(IRN) is not a simple reflection nebula. The wavelength dependence of polarisation is mathematically treated and compared to known values, following Serkowski's empirical relationship. Possible configurations of the nebulosity are discussed and interpretations suggested.

# CONTENTS

# LIST OF FIGURES

# PREFACE.

The contents of this thesis describe some of the work carried out by the author, under the supervision of Dr. S.M. Scarrott. Although the author was not involved with the design and development of the polarimeter, it is necessary to include a brief description as it gives a more complete picture of the instrumentation.

No part of this thesis has previously been submitted for a degree in this or any other university, and the work is due to the author unless otherwise acknowledged.

# CHAPTER ONE
# INTERSTELLAR GAS AND DUST

## 1) INTRODUCTION

Interstellar material constitutes as much as ten per cent of the total mass of the Galaxy, and is also present in the spiral arms of other galaxies which are comparable to our own. The term "nebula" has been used to refer to many of the clouds composed of interstellar material, and such nebulae can be described as being either "dark" or "bright". The dark nebulae, for example; the Horsehead nebula in Orion, obscure the light from more distant objects. Bright nebulae are luminous, for example; M42 in Orion, seen by gaseous emission and scattered starlight.

Other evidence for interstellar material is varied. With bright nebulae, the evidence is direct, but other evidence (such as radio emissions from molecular and atomic transitions, interstellar absorption lines, and interstellar extinction and reddening) is convincing and infers the presence of large quantities of gas and dust.

Interstellar clouds are believed to be composed of gas, mainly hydrogen and helium, since these are the most abundant elements in the universe, but atoms of other elements are also present. To explain certain evidence, it is now believed that some of the clouds have a component of solid particles

known as "grains" or "dust". It is these solid particles which extinguish the light from background objects, and much interest lies in understanding their origin, composition and processes involved. The relatively large size of the grains make the particles efficient scatterers and absorbers of light. The efficiency of the scattering by the grains is dependent on their size, particularly when particle size is comparable to the wavelength of the light. The wavelength dependence of the extinction of starlight suggests that interstellar grains have dimensions which are approximately that of visible wavelengths ( 0.4 to 0.7 microns). To account for the observed levels of such extinction, (approximately 0.5 magnitudes per kiloparsec within the galactic plane), we would only need approximately 1 grain in $10^{13}$ cubic centimetres of space.

In general, it is believed that 1 per cent of the mass of interstellar material is vested in the grains or dust, and the remaining 99 per cent is composed of gas. This figure was originally derived from the ratio in the solar neighbourhood. Oort used this value to deduce the mean density of the interstellar dust perpendicular to the galactic plane. He then measured the combined density of stars and gas in the solar neighbourhood to be $6 \times 10^{-23}$ kg per cubic metre. Van de Hulst (1981) obtained a value of $1.4 \times 10^{-25}$ kg per cubic metre from 21 cm observations.

Given that the grains are so finely distributed - with on average only one grain in a hundred metre cube, it is surprising that they should have any significant effects whatsoever. However these grains are of considerable importance, and following Morton's measurements of interstellar extinction (1974), Greenberg deduced an extinction due to dust of two magnitudes per kiloparsec in the vicinity of the Milky Way (1975). The interstellar reddening is the most obvious way in which the interstellar dust betrays its presence. As starlight passes through dust clouds, a certain amount of energy is removed from the incident light by the grains so that the intensity of the starlight is reduced. The absorbed energy can then be re-radiated as infrared, while the majority is re-emitted at the original wavelength (scattering).

The amount of extinction is dependent upon the chemical constitution of the scattering materials, as well as the size of the grains. Generally, with

metallic particles, the absorption is large compared to the scattering, whereas with dielectrics, extinction is mainly by scattering. It seems obvious to assume that there should be significant variations in the composition of dust particles form different regions, as the physical environments of the grains can be markedly different, e.g; dark clouds have temperatures of between 5 and 20K, whereas HII regions have temperatures of around 10,000 K.

## 2) CLASSIFICATION OF NEBULAE

The term "nebulae" has come down through the centuries as the name given to permanent cloudy patches in the night sky, which are beyond the solar system. A few nebulae had been known to naked eye observers, and with the development of the telescope, more of these nebulae were found. Sir William Herschel (1738-1822) carried out research on nebulae and catalogued 2,500 such objects. As telescopes improved, however, many of the then known nebulae became resolved into star clusters, a situation which led Herschel to propose that all such nebulae could be resolved into star clusters, if the telescopic power and resolution were available.

Messier published catalogues of nebulae, the last and most famous of which contained 103 of the most conspicuous nebulae of the time ( 1784 ), e.g. the Crab Nebula is designated as M1.

In 1912, Barnard attributed dark nebulae to obscuring dust clouds, and Sir William Huggins ( 1824-1910 ) used a spectrograph to demonstrate that some of the bright nebulae were composed of luminous gas. By this time, those nebulae which could be resolved into star clusters had been weeded out of the lists to form a separate study. It was also recognised that nebulae could be divided into two types

### 2.1) Galactic nebulae

This type was found within the Milky Way, i.e. members of our galaxy, for example, the great nebula in Orion, known as M42. They retain their diffuse nature even with the most powerful of telescopes. They are believed to be composed of clouds of gas and fine particles and are varied in form.

## 2.2) Extra-Galactic nebulae

These are nebulae which are found in regions of the sky outside the Milky Way, e.g. M31 which is now known to be the Andromeda galaxy. However, the distances of the nebulae were unknown and beyond the limits of the techniques established at the time. It is now known that extra-galactic nebulae owe their diffuseness to their remoteness. It is believed that many of them are galaxies similar to the Milky Way, comparable in size and dimensions.

## 3) GALACTIC NEBULAE

Galactic nebulae can be further sub-divided into groups such as

## 3.1) Planetary Nebulae

These are usually more or less circular or annular in appearance, with well defined edges. Through a telescope they vaguely resemble planets, hence their name. This type often shows a star at the centre, e.g. the ring nebula of Lyra (NGC 6720). It is believed that the ring nebula is a shell of expanding gas seen in projection, ejected by a star within the ring. Less than 400 planetary type nebulae are known, and their apparent diameters are, in general, less than one arcminute.

## 3.2) Diffuse or Irregular Nebulae

These have no well-defined shape and the contours are blurred or serrated. This type are more numerous than the former type, but have a different spatial distribution; planetary nebulae are more commonly observed within the galactic plane, particularly towards the direction of the centre of the Milky Way.

Another way of classifying bright nebulae is according to their spectra. Bright nebulae fall within two distinct groups:

## 3.3) Emission Nebulae

This type is so-called because the nebulae show emission-line spectra e.g.

the Orion M42 nebula. Such nebulae are composed of gas, with the constituent elements identified by the spectrum. The main gas is hydrogen, but other elements such as helium, oxygen, nitrogen are to be found. Within or near an emission nebula, one or more very hot stars (with temperatures greater than 20,000 k ) can be found, and it is believed that energy from these stars is absorbed by the gas and then cause ionisation to produce the observed spectral features of the bright nebula. The intense ultra-violet radiation from the star ionises all of the hydrogen atoms in its neighbourhood, the extent of the ionisation of the surrounding gas being dependent on the density of the gas, and also upon the temperature and luminosity of the star.

These regions of ionised hydrogen around hot stars are referred to as HII regions. Within these regions, there are some proton which recapture electrons, and it is from these that the emission line spectrum of hydrogen is formed. After an electron has been re-captured, the atom quickly loses energy by emitting light and returning to its ground state. The U.V. energy from the nearby star is so strong, however, that the hydrogen atom will quickly be ionised again. Throughout the nebula, there are sufficient re-combinations at any time to make the cloud glow brightly.

## 3.4) Reflection nebulae

This type of nebula actually reflects the light of a nearby star. The nebulosity surrounding the Pleiades is an example. These clouds show a similar, but slightly bluer colour than that of the illuminating star, so it is believed that such nebulae are composed of material which reflects light from a central star.

Several hundred reflection nebulae have been identified so far, and have been tabulated in catalogues by Cederblad (1946), Dorschner and Gurtler (1966), and Van den Burgh (1966). Racine (1968) extended the catalogue with extensive photometric and spectroscopic observations of the listed stars.

Reflection nebulae are not a uniform category of astronomical objects, and they do not seem to be uniformly distributed throughout the galaxy. They can be subdivided into three sub-groups;

1) Compact objects, where the associated dust and gas is connected to an illuminating star.
2) Larger objects, where the dust and gas seems to be part of an extensive molecular cloud.
3) Objects to be found at a high galactic latitude, which do not seem to have obvious illuminating stars.

This latter group were studied by Van den Bergh (1966), who observed that the majority of these objects were located south of the galactic plane, towards the galactic centre. It was thought that most of these objects were shining by reflection of the integrated light of the galactic centre.

Early work on reflection nebulae was greatly affected by systematic errors in equipment and techniques. However, research has proceeded with studies of surface brightness, colours and polarisation in various wavelengths, not just in the visible range, but in ultra-violet, infrared, and radio wavelengths.

Spectroscopic observations of reflection nebulae by Struve at Yerkes Observatory (1936) gave the results that reflection nebulae were generally bluer than the associated illuminating star, although this conflicted with work by Keenan (1936), who studied NGC 7023, and found it to be more luminous towards the red end of the spectrum.

The issue was clarified in the late fifties, when Martel produced data on seven nebulae, showing that all were slightly bluer than the associated illuminating stars. Later work confirmed this further, but also found that although reflection nebulae generally were bluer than the illuminating stars, the nebulae tended to redden with distance taken into account.

Originally, several ideas were proposed; scattering by atoms is not plausible because a very high density of atoms would be needed to scatter the light. Scattering by molecules was also ruled out, because molecular scattering is selective of blue light ( e.g. in Earths atmosphere, molecular scattering is what causes the sky to appear blue.)

The scattering must be due to particles larger than molecules, which are often described as "dust". If we compare the total light scattered by the nebula, to the light radiated from the central star, we find that the particles reflect a

large percentage of the light incident upon them. Since hydrogen is the most abundant element, it led to the suggestion that such particles could be frozen compounds of hydrogen, such as ice, methane or ammonia, where the particles are about a few tenths of a micron in size.

It has been known from the early forties (Baade, 1944), that there was a connection between young early-type stars and interstellar clouds. However the suggestion of a direct generative link between such stars and reflection nebulae was disputed. At the time of Cederblad's catalogue, there was no significant connection between the distribution of diffuse nebulae and that of stars of any stellar type. However, more recent theories of star formation have tended towards natural mechanisms from which reflection nebulae may be expected to develop.

## 4) COMETARY AND BIPOLAR NEBULAE

These have a distinctive visual appearance of arcs or fans of nebulosity associated with individual stars. Current ideas about their structure suppose that radiation and matter from the stellar surroundings are collimated by circumstellar material, which is perhaps in the form of a disk or torus, to flow outwards in one or two diametrically opposed directions, to give the characteristic bipolar nebula shapes. Bipolar nebulae have two distinct lobes of nebulosity, which are centred upon an illuminating star. This star could be in the post-main sequence phase, e.g. the Boomerang Nebula (Taylor and Scarrott, 1980).

Cometary nebulae are single lobe nebulosities associated with stars, and there appears to be a wider variation in structure than with the former type. The lobes can be in the form of, say, narrow arcs or a fan of nebulosity. Cometary nebulae are found in association with pre- main sequence stars only. The orientation of the circumstellar torus is quite crucial, as its position with respect to the observer leads to the various apparent nebulae shapes. Stars in cometary nebulae are often seen
as condensations or "knots", as opposed to regular stellar images, and this is

probably due to heavy obscuration around them.

It has been suggested that cometary nebulae and pre- main sequence bipolars are really just the same phenomenon, and the difference could be due to one of the lobes being obscured, or the viewing angle of the observer.

# CHAPTER TWO
# THE POLARISATION OF LIGHT

## 1) INTRODUCTION

The polarisation of light was discovered by Christian Huygens in 1690, while working with calcite and developing his wave theory of light. At the time, however, his ideas were in conflict with Isaac Newton, who believed that light was, in fact, comprised of corpuscles, or particles.

The wave theory of light was taken up by Dr. Thomas Young (1773 -1829) who developed the principle of interference of light. In 1803 he explained the phenomenon of coloured fringes seen in thin films using wave theory, although it was not popular as it was again in conflict with Newton's work.

It was not until 1816 when Augustin Jean Fresnel (1788 - 1827) gave the first theoretical model of polarisation, that the wave theory began to be accepted. Dominique Arago, collaborated with Fresnel, and he found that the sunlit sky was partially plane polarised.

In developing the wave theory of light, it was established that light was a transverse electromagnetic wave. Michael Faraday (1791-1867), believed that there was a physical inter-relationship between electromagnetism and light, and this was developed further by James Clerk Maxwell (1831-1879), who gave a mathematical description of electromagnetic waves.

There are two general types of wave, longitudinal and transverse. They differ in the directions which the vibrations or displacements occur with respect to the direction of propagation of the wave. A longitudinal wave occurs when the particles of the medium are displaced from their equilibrium position in the same direction as the wave, whereas a transverse wave arises when the disturbance, or displacement is perpendicular to the wave motion.

Classically, light can be considered to be a transverse electromagnetic wave, where the vibrations are perpendicular to the direction of propagation of the wave. All electromagnetic waves have two vectors, an Electric vector (E) and a magnetic vector (B), which are both perpendicular to each other, as well as to the wave direction, as indicated in the diagram below.

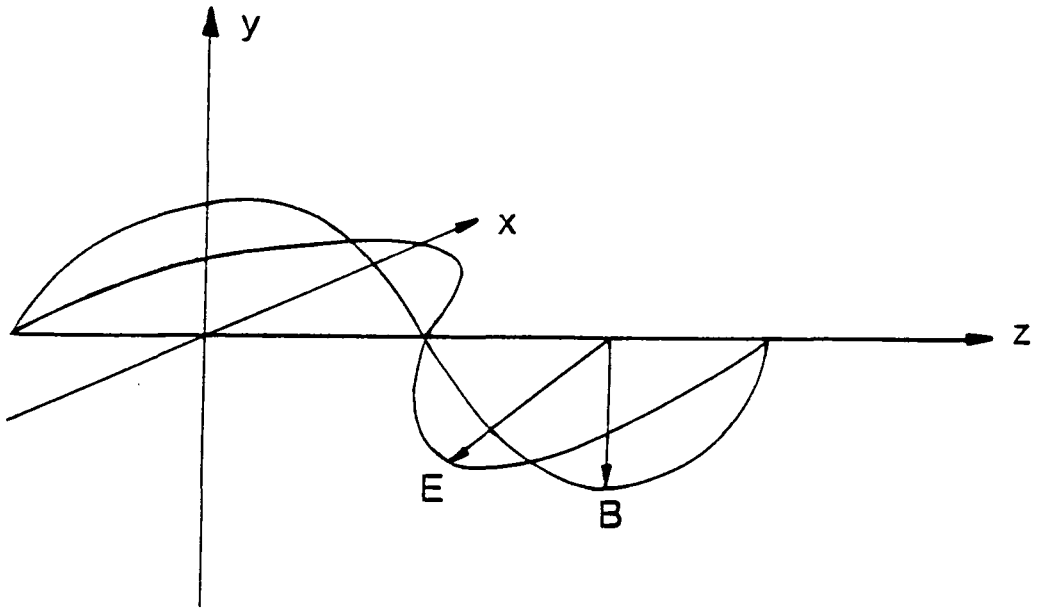


When the orientation of the Electric field (E) remains constant, (although its magnitude and sign will vary with time), it is said to be plane polarised, or linearly polarised. The electric field therefore resides in the "plane of vibration", which contains the Electric field vector (E), and the direction of propagation of the wave (k). Normal unpolarised light can be regarded as a superposition of a large number of plane polarised waves, with random phase shifts and orientations which causes the plane containing the E-vector to vary with time.

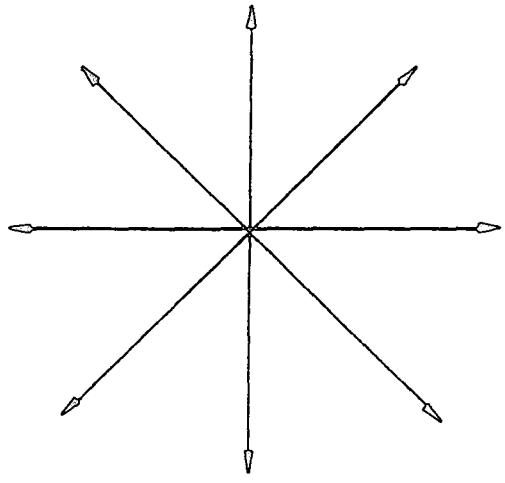

unpolarised light

Partially polarised light can occur when the electric vector (E) shows a preference for a particular direction, and in this case the degree of polarisation is defined as the ratio of the intensity of the polarised component to the intensity of the whole beam. If we have two harmonic, linearly polarised light waves, of the same frequency, moving in the same direction, then if the two electric field vectors are co-linear, the superimposing disturbances will combine to form a resultant linearly polarised wave, of which the amplitude and the phase can be calculated.

However, if the two light waves are such that their electric field directions are perpendicular, the resultant wave may not be linearly polarised. The superposition of waves may result not just in linear polarisation, but in particular cases of circular or elliptical polarisation. Generally, light, whether natural or artificial, is partially polarised to some degree, with the cases of total polarisation or unpolarisation as extremes.

## 2) METHODS OF PRODUCING POLARISATION.

Light can be polarised by various physical mechanisms; dichroism or selective absorption, reflection, scattering, and birefringence (double refraction). In the subject of astronomy, however, we are interested in how light from

astronomical objects can be polarised, (both linear and circular polarisation can be considered, and are both of importance), and also if the light is polarised at the source, or in transit between the source and the observer.

Preferential absorption is the mechanism in which aligned non-spherical grains can absorb one component of a beam of unpolarised light, to a greater extent than the other. This is thought to be due to a magnetic field present throughout the region. The component of light which is parallel to the grains, and perpendicular to the direction of the field, will be partly absorbed, and the light seen through the region will be partially polarised parallel to the field. This is the basis of the Davis and Greenstein mechanism, which will be discussed in greater detail later.

The process of scattering is also of interest to astronomers, and this is where light can be scattered from electrons or dust particles, and result in partial polarisation of the incident light. The cross-section of an electron is so small, however, that for most interstellar electron densities, the majority of the incident light passes through unaffected, and hence, unscattered, so the resultant percentage polarisation is minimal, and the intensity is low.

Unpolarised light which is incident upon dust grains, can be scattered and the light will then be partially polarised in the direction perpendicular to the plane of scattering. This mechanism can enable astronomers to examine dust clouds, and determine the illuminating source of the light. In some cases, for example, the polarisation pattern for a dust cloud may be centro-symmetric about a particular source. On the other hand, the light may appear to be polarised and show a particular polarisation pattern, due to the non-spherical geometry of the associated dust cloud.

## 2.1) Scattering

The scattering of light from particles has been treated mathematically for various conditions. The treatment of infinitely small particles is considered in "Rayleigh scattering", where the size of the particles is significantly less than the wavelength, while infinitely large particles are considered in "Geometric scattering". The first solution for particles of arbitrary size was derived by Mie

(1908), for the case of smooth homogeneous spheres. Since then, other more elaborate methods have been applied to special considerations of the geometrical shape, e.g. ellipsoids and cylinder shapes (Van de Hulst, 1981). From observations of interstellar polarisation, it seems that the grains are not perfectly spherical, but as long as the degree of ellipticity is small, then Mie calculations give an adequate approximation to light interaction with the interstellar grains.

The mathematical treatment of Mie scattering involves the wavelength of the radiation, the radius of the scattering particle, and the value of its complex refractive index. Scattering may be represented by the equation;

$$S_S = M(\alpha) S_i$$

Where $S_i$ and $S_S$ are the incident and scattered Stokes Vectors (with components I,Q,U,V). M is the scattering matrix and $\alpha$ is the cosine of the scattering angle.

The scattering properties of a sphere of radius, "a", for plane polarised radiation of wavelength $\lambda$ may be determined by;

$$x = \frac{2a\pi}{\lambda}$$

$$m = n - ik = \sqrt{\left( K - \frac{2i\sigma\lambda}{c} \right)}$$

where n and k are the refractive and absorptive indices, K is the dielectric constant, and $\sigma$ is the conductivity of the particle material. A scheme for actually evaluating the Mie functions is given in Wickramasinghe (1973) and has been implemented by Warren-Smith (1979, 1983). The scattering functions of a single sphere, as calculated from Mie theory, show a diversity of

forms depending upon the size and refractive index of the sphere.

To use Mie's scattering theory to represent the scattering of light by interstellar dust grains, we must average the scattering functions for a single sized sphere over the range of sizes found amongst the dust grains. To do this averaging, we assume the dust grains have a range of sizes with a distribution function of n(a), such that the probability of a grain having a radius of between a and a+δa is n(a). It is normalised so that;

$$\int_{a\min}^{a\max} n(a)\,\delta a = 1$$

By integrating over the total range, we can then find the average cross sections for the grains ( see Warren - Smith)

## 2.2) Polarisation by aligned grains.

In 1949, Hall and Hiltner discovered interstellar polarisation during searches for intrinsic polarisation in early-type stellar atmospheres. For polarisation as well as extinction to occur, the particles or "grains" of interstellar dust must be aligned in some way. Optical observations of thousands of early-type stars showed that the degree of linear polarisation was proportional to the extinction occurring.

The starlight that passes through an interstellar cloud is usually polarised in some way by the dust grains. For this to happen, the grains must be non-spherical, possibly rod-like or flake-like in shape, and aligned uniformly over large distances. The only plausible mechanism for such alignment is the very weak magnetic field of our galaxy. However, to interact with a magnetic field, the grains must be weakly magnetic themselves.

Davis and Greenstein proposed the paramagnetic relaxation process in 1951. It was clear that the grains were not aligned like compass needles along the magnetic field lines, because if there were any impacts by the interstellar gas atoms, then this would knock the whole system out of order, quicker than the field could re-orientate the grains.

Instead, it is believed that the grains are spinning at up to 100,000 times per second, set spinning by collisions with molecules from the interstellar gas. There is a resultant torque which aligns the grains so that their long axes are perpendicular to the field. (see figure 2.1)

The question of alignment, and the mechanisms required to produce it has generated much research and interest. The paramagnetic relaxation mechanism is favoured, and used as a base for further considerations. According to this model, when a grain spins in the magnetic field, every part of the grain "sees" a sinusoidally varying magnetic field, unless the motion is perpendicular to the field direction. Due to magnetic relaxation, the induced magnetisation is slightly out of phase with the inducing field, and this results in a torque. This torque raises the internal energy of the grain, but the grain radiates away this energy, so it does not raise the temperature of the grain. As the grain temperature is less than the spinning temperature (due to collisions with the gas), this makes alignment possible. If the temperatures were the same, however, then a much bigger magnetic field would be required. (The maximum magnetic field is approximately $5 \times 10^{-6}$ gauss.)

To examine the polarising properties of interstellar dust grains, their shapes may be approximated to ellipsoids or long cylinders. Van de Hulst (1950) estimated that polarisation produced by prolate spheroids with an axis ratio of 1:2 would be half of that produced by long cylinders. The cross-sections for ellipsoids were calculated by Greenberg in 1960. The wavelength dependence of interstellar polarisation was investigated by Hiltner in 1949.

The comparison of observed wavelength dependence of interstellar polarisation and extinction, with the values of the cross-sections of dust grains (obtained by Greenberg and Van de Hulst) was made by Serkowski (1962). The general conclusion is that the observed wavelength dependence of polarisation and extinction can be explained assuming dielectric, elongated dust grains, which would have a refractive index of not less than 1.4, and diameters of about 0.3 microns.

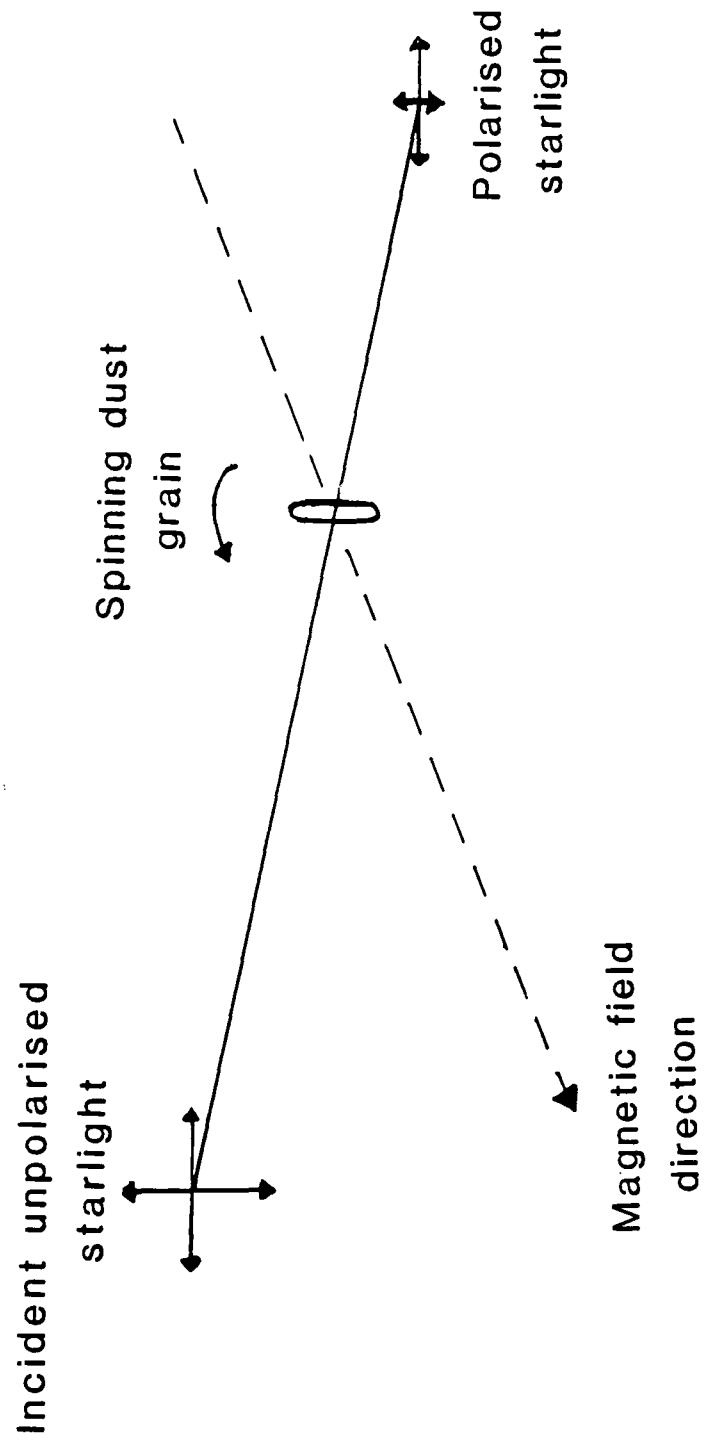


Fig. 2.1 Davis and Greenstein mechanism

## 2.3) Serkowski's relationship

The wavelength dependence of interstellar linear polarisation over optical wavelengths (0.30 -1.00 μm) was first noted by Gehrels (1960). The wavelength dependence of polarisation was plotted for a number of stars by Coyne and Wickramasinge (1969). They found the general shape of the curve to be fairly consistent with a polarisation maximum at a reciprocal wavelength ($\lambda^{-1}$) approximately 2 $\mu m.^{-1}$

It was also found that even for stars with varying polarisation as a function of wavelength, there was a high degree of uniformity found by plotting P/Pmax against $\lambda_{max}/\lambda$, where $\lambda_{max}$ and $P_{max}$ are the wavelength and the value of the polarisation at the maximum.

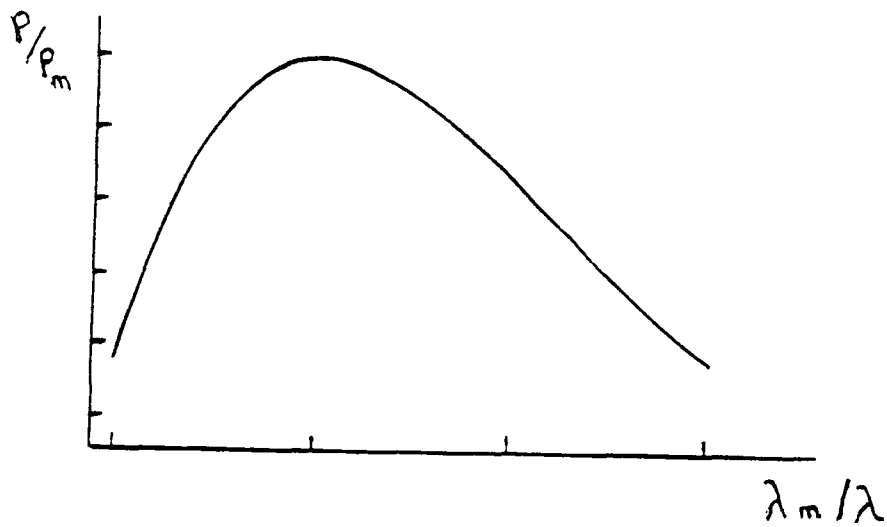


The empirical relationship between polarisation and wavelength is given by the equation;

$$P(\lambda)/P_m = \exp(-1.15\ln^2\{\lambda_m\}/\{\lambda\})$$

Serkowski and Robertson (1969) studied the wavelength dependence of polarisation, and examined several regions of the sky. They found that some sources had values of $P_{max}$ which were significantly higher or lower than average, and suggested that the wavelength dependence of polarisation was an indicator of variations in the size of the interstellar dust grains.

Since then it has been shown to be quite effective for investigating various properties of the interstellar medium, particularly following two rather extensive studies: Coyne, Gehrels and Serkowski (1974), and Serkowski, Mathewson and Ford (1975)

## 2.4) Other alignment mechanisms.

The alignment of dust grains by interaction with gas flowing in a direction perpendicular to the galactic plane was suggested by Gold (1952). In his proposals, the long axes of the grains tend to be parallel to the relative velocity, and the alignment would be with the long axis normal to the direction of relative motion. Davis, however, showed that the alignment of dust grains in this would be too small to explain the observed polarisation.

The theory of alignment of ferromagnetic grains by a strong magnetic field was discussed by Spitzer and Tukey (1951). In a strong field, the torque on the ferromagnetic grains will stop the spinning of the grains, and they will be aligned as compass needles with their long axes parallel to the magnetic field. For this to occur, the magnetic field must be perpendicular to the galactic plane.

Purcell's pinwheel alignment mechanism must also be considered, where the grains spin at high angular velocities due to inhomogenities on the surface of the grain, which results in a mean torque with respect to an axis fixed in the grain. Such torques arise when atoms (such as Hydrogen) collide with the grain and stick to it.

Hollenbach and Salpeter (1971) suggest a limited number of possible sites exist on such a grain, and are simply impurities or surface defects, but serve to catalyse the formation of molecular hydrogen. A torque can also be the result of a variation in the photoelectric emissivity or the accommodation

coefficient ( i.e the fraction of gas-atom kinetic energy transferred to the grain in a gas-grain collision.)

These processes produce relatively strong systematic torques, leading to frequencies as high as $10^9$ $s^{-1}$ corresponding to rotational velocities ($a\omega$) of $10^4$ cm $s^{-1}$ for a grain of 0.1 micron. Purcell also showed that in the presence of dissipative processes, the grain's angular momentum direction will lie along the principal moment of inertia.

Grain growth is subject to certain limitations, as small particles or clusters are not as stable as bulk material. Below a certain critical cluster size, the clusters are more likely to evaporate than grow. Salpeter (1977) investigated the depletion of the vapour by cluster nucleation and growth, and assumed that the vibrational temperature of the clusters, and the kinetic temperature of the gas were the same. He also suggested that the actual grain formation may take place within the cooler patches of stellar regions.

## 3) POLARISATION OF ASTRONOMICAL OBJECTS

Stokes, in 1852, described the four Stokes parameters, and in 1908, Mie and Debye developed the theory of light scattering from small particles. In 1949, Hall and Hiltner discovered interstellar linear polarisation, and did extensive research in this field. The polarisation of nebulae and other astronomical objects has generated great enthusiasm, and enabled wider information and understanding of stellar processes.

Polarised radiation has been detected at a wide range of wavelengths, e.g. at radio wavelengths from both galactic and extra-galactic sources, at infrared wavelengths from protostars, and at optical wavelengths from reflection nebulae and from planetary atmospheres. Consequently, in recent years the study of the polarisation of light from astronomical objects has become a very important area of current research in astronomy.

Polarisation studies of reflection nebulae began with observations of NGC 2261 - Hubbles variable nebula, by Meyer (1920). Despite early problems due to the large errors involved, it was clear that polarimetry would be of great use to astronomers.

Elvius and Hall, (1966) examined NGC 2068, and by their polarisation studies, they were able to show that of the two prominent stars in the vicinity of the nebula, only one of them was, in fact, associated with the illumination of the object. The polarisation vectors produced a centro-symmetric pattern, which is characteristic of polarised light from a single source illuminating dust by reflection.

The same procedure was applied to the bipolar nebula S106 (Perkins, King and Scarrott, 1981) to identify a completely obscured optical source, which is associated with a prominent infrared feature.

It can be seen that polarisation studies of astronomical objects can extend knowledge and understanding considerably, and give information on nebular structures, grain size and composition, and insight into the presence and form of magnetic fields.

# CHAPTER THREE
# POLARISATION DISCS AROUND YOUNG STARS.

## 1) INTRODUCTION

Circumstellar discs play a very important role in active star formation, and the associated phenomena such as stellar jets, bipolar outflows, etc. These discs are primarily investigated by studying their molecular line emission, as there is little direct evidence for them at optical wavelengths, but more information is obtained by studying their infrared emission.

However, in the optical polarisation studies of various reflection nebulae, and other similar objects, some of the deviations occurring in the expected patterns of the polarisation suggest the presence of circumstellar discs. Such deviations, which have come to be known as polarisation discs, can be seen in cometary nebulae, bipolar nebulae, and systems with stellar jets, which are related to regions of star formation and mass outflows.

Some of the properties of polarisation discs are;

1) The polarisation disc consists of an anomalous band of polarisation, which can be found near the apex region of conically shaped reflection nebulae. The polarisation band is present, regardless of the visibility of the central source.

2) If the central source is directly visible, then it is linearly polarised in a similar orientation to the disc. However, the position angle of the linear polarisation varies with wavelength.

3) If molecular bipolar outflows are present, then the polarisation disc is perpendicular to the axis of the outflow.

4) If small stellar jets are present, then it is found that the inner part of the jet, and the source, are polarised with orientations perpendicular to the jet axis.

5) At the extremities of the polarisation disc are null points.

6) The polarisation disc may change its orientation with time.

Although it seems likely that the polarisation discs are a consequence of the circumstellar shells, the actual mechanism giving rise to such phenomena is less easy to explain. The properties of these discs, as outlined above, suggest a possible explanation.

Firstly, the disc can not arise from the single scattering of unpolarised light from a central source, because the pattern of vectors lacks the required centro-symmetry. Secondly, we have competing polarisation mechanisms, which can fully cancel in some regions to produce null points, on either side of the central object, and co-linear with it. These mechanisms are also responsible for the wavelength dependence of the position angle and level of linear polarisation. There are several models which have been suggested to explain the formation of polarisation discs;

## 2) MULTIPLE SCATTERING MODELS.

If the polarisation disc is optically thick, then the radiation which emerges may have been multiply scattered. The resultant polarisation pattern should still be

centro-symmetric, but the level of polarisation would be reduced.

Bastien and Menard developed a model (1988), in which the disc is so dense that it is opaque along its equatorial plane and radiation can only escape along the polar axis of the disc. The emerging polar radiation is then scattered by the lobes, which are optically thin, and this leads to the illumination of the edges of the disc, where it is scattered again. Therefore we have a double scattering effect, which could produce the band of polarisation observed. However, the model does not explain how the central object can be polarised on a par with the surrounding disc.

## 3) ELSASSER AND STAUDE MODEL.

This model considers a central stellar source embedded symmetrically in a disk-like configuration of dust and gas, surrounded by a tenuous cloud. (See figure 3.1). The optical thickness of the disk is relatively large, and an observer viewing the disk nearly edge-on will see highly polarised scattered light from the optically thin polar regions, which is superimposed upon the highly attenuated unpolarised direct light from the central star. (See figure 3.1 (A)).

At wavelengths of maximum extinction, the unpolarised direct light is diminished, whereas the contribution from the optically thin cloud remains nearly unchanged, which then gives rise to an increase of the net polarisation with increasing optical depth.

Configurations of this kind are believed to be supportive of the bipolar nebula and compact HII regions, e.g. S 106 (Eiroa et al, 1979 ), which have been spatially resolved. Strong linear polarisation in the polar lobes, which is orientated parallel to the equatorial disk, has been observed in several objects of this type, e.g. the Egg nebula and Minkowski's footprint (Schmidt et al. 1978).

Besides possible obstruction by foreground extinction, the distance of the objects may prevent clear resolution. Structures more compact than that of the bipolar nebula model can be imagined, e.g. a compact circumstellar shell disrupted at the poles, which would give rise to the same polarisation effects, and may have diameters which are smaller than that in the previous diagram.

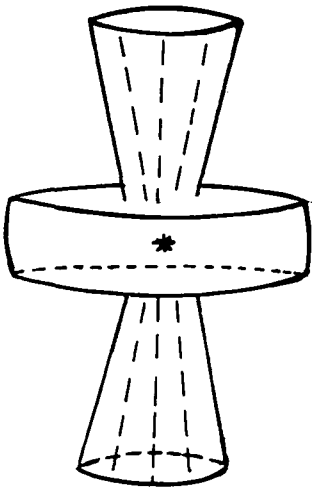


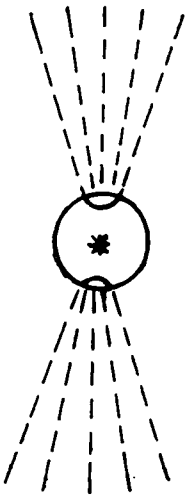


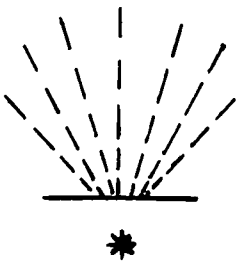


**Elsasser and Staude Model**

Fig. 3.1

(See figure 3.1 (B).)

In both cases, the shape of the object leads us to consider rotation. Lucas et al (1978) established that the axis of rotation of the molecular cloud embedding S 106 is parallel to the symmetry axis of this compact HII region.

A third configuration may also be considered, where a star is hidden behind a sharply bound obscuring edge ( blister object), as in figure 3.1 (C). This is equivalent to the former cases, with respect to the resulting polarisation observed. However, a relationship between the direction of polarisation and the stellar angular momentum is not developed in this model.

Elsasser and Staude stress that the interpretation of the polarisation observed does not depend upon the geometrical details of the models, although the existence of a steep density gradient, or density step, in one direction from the illuminating source is found. They have shown that scattering by circumstellar dust and electrons, which is distributed in a non-spherical way, can account for the large polarisation which is observed in a variety of young stellar objects.

## 4) THE POLARISED SOURCE MODEL.

This model suggests that the apparent central source emits light which is linearly polarised, but is then scattered by dust grains within the circumstellar disc. The model is a development from the previous Elsasser and Staude model, in the context of cometary and bipolar nebulae by Notni (1985), and for the NGC 2261 / R. Mon. complex by Draper (1988).

The origin of the polarised source needs explanation, and it is possible that the dust which is surrounding the source is asymmetrically distributed, and therefore the light which is scattered from this dust then illuminates the more extensive circumstellar disc to give rise to the observed effect. The apparent polarisation of the central source can vary with time, as long as the asymmetric illumination is restricted to small distances from the central source.

## 5) THE MAGNETISED DISC MODEL.

In this model, it is proposed that the circumstellar disc contains magnetically

aligned grains, which are non-spherical in shape. These grains modify the polarisation of the light by dichroic or selective extinction, and this leads to two competing polarisation processes; scattering and extinction. The competing mechanisms then produce cancelling effects i.e., null points, and the wavelength dependence of the level and orientation of the polarisation of the disc and the central object.

The model requires that there is a toroidal magnetic field within the disc, which aligns the grains. However, magnetic alignment of dust grains is a relatively slow process, and it difficult to see how reorientation of the polarisation disc over short periods (e.g., few years) is possible. This model is also used to explain the fact that the polarisation tends to align itself with the bright rim of the nebulosity.

The polarised source and magnetised disc models can both be used to explain most of the observed features of polarisation discs, but neither of them can be used exclusively, as neither model explains all of the features in all of the objects. It is therefore accepted that some objects have polarised sources while others have magnetised discs, or perhaps, a combination of the two models, which was suggested to explain the polarisation disc in NGC 2261 / R.Mon. by Scarrott et al. (1988). The interpretations of the physical processes which give rise to the polarisation discs are quite complex. The interpretations, however, would be facilitated by accurate measurements of the wavelength dependence of polarisation in the discs and central sources.

## 6) THE POLARISATION DISC IN NGC 2261

The linear polarisation of NGC 2261 was studied extensively by Scarrott, Draper, and Warren-Smith continouously over a period of years. They found that the orientation of the polarisation disc had changed dramatically in the time space of one decade. They suggest that this is due to the scattering of radiation within a dust/gas circumstellar disc from a central source which is emitting polarised light. There is also the possibility of subsidiary effects due to extinction by magnetically aligned grains in the larger interstellar disc which is surrounding R. Mon.

The system is tilted to our line of sight in such a way that the northern outflow is directed towards us, and this corresponds to the optical nebula. The southern optical nebula is obscured by part of the disc, although a faint streak of nebulosity which emanates in a south-westerly direction is believed to be associated with it. The presence of a large scale disc surrounding R. Mon. can be inferred from molecular line studies, but imaging polarimetry in optical wavelengths also indicates the presence of the disc. The disc can be detected from the array of parallel polarisation vectors which are centred on the star. The polarisation maps which were produced showed the presence of bands of polarisation across the head of the nebula, including the illuminator R. Mon. The orientation of the polarisation disc can be determined from the polarisation of R. Mon. and the null points to the east and the west of the star. From the maps, it is clear that the orientation of the polarisation disc changed by approximately $20^{o}$ between 1979 and 1981.

The overall pattern of the polarisation over NGC 2261 suggests that the system is much more complex than a simple reflection nebula. The polarisation disc is changing its orientation with time, on time scales of months/years. It is interpreted as an initially polarised source model; Extinction by magnetic grains is not a viable mechanism for explaining the polarisation disc, and it seems more likely to be scattering of initially polarised light. However, it is believed that extinction could produce additional effects within the interstellar disc, and the net effect of the two mechanisms will give rise to the observed polarisation patterns, null points, wavelength variation in the polarisation and the associated brightness changes.

# CHAPTER FOUR
# A REVIEW OF NGC 2264

## 1) INTRODUCTION

NGC 2264 is an open star cluster of extreme youth associated with diffuse nebulosity, situated in front of an extensive dark cloud in northern Monoceros. Although NGC 2264 appears in the sky to be near the Rosette nebula, the latter is much more distant, and there is no physical connection. As well as very young stars, the region has emission nebulosity and dust clouds. The young open cluster referred to as NGC 2264 is about 1.3 degrees square and situated within a bright extended HII region. Adams, Strom and Strom (1983) calculated the distance of NGC 2264 as approximately 800 parsecs and the angular size of the cluster to be of the order of 35', when they made observations of NGC 2264 in 1983. They selected to study this nebula in detail as they believed it to be a site of low-mass star formation; it is a relatively populous cluster with pre-main sequence stars of absolute magnitudes form 7.5 to 12.5, which is a luminosity range over which young stellar objects merit further investigation.

The cone nebula lies to the south of NGC 2264. It is a diffuse nebula which is believed to be an area of both recent and continuous star formation. In the past decade, attention has been directed towards the region near the cone

nebula, which contains Allen's Infrared object GL989 (Allen 1972), and a very small nebula. It is this small "knot of nebulosity" that is of particular interest in this study, and will be referred to as the Cone IR Nebula (Cone IRN). The diffuse nature of the nebulosity can be seen in the photographs, and the coneIRN lies to the south of the larger nebula, (see plates 4.1 and 4.2). The photographs show the region in increasing magnification and were taken from the Mount Palomar sky survey prints.

There is considerable mass in the molecular clouds associated with NGC 2264, which has not, as yet, condensed into stars. Crutcher, Hartkopf and Giguere (1978) found that the NGC 2264 molecular complex consists of at least six distinct clouds, with a total mass of $2 \times 10^4$ the mass of the sun. The mass of the stellar population is only approximately 20 percent of this value (Walker 1956), so it could be that this molecular material could be forming stars at the moment.

Data suggest that star formation in the NGC 2264 complex has proceeded for at least $10^7$ years (Adams, Strom and Strom, 1983), which is consistent with their previous estimates, (Warner, Strom and Strom, 1977). Adams, Strom and Strom presented the results of a photometric study of the stellar population in the NGC2264 region, with particular interest in low mass stars ( $< 0.5 M_\odot$ ), and determining the star-forming history of the region. The peak rates of star formation were reached at different times for stars of different masses. Low mass stars, i.e. stars with mass of less than half of the mass of the sun appear to form first, whereas the peak rate of star formation for greater masses is not reached until later in the evolutionary history of the cloud complex. This was in agreement with earlier work by Iben and Talbot (1966). (The idea of co-eval star formation in open clusters had been unchallenged until the early 1960's, when Herbig (1962) was among the first to consider that different masses formed at different times - i.e star formation was not initiated instantly at all masses.) Iben and Talbot (1966) also found evidence for an age spread in NGC2264 as well, and furthermore suggested that the star formation rate in this cluster has increased exponentially with time.

There is still considerable mass in the molecular clouds associated with

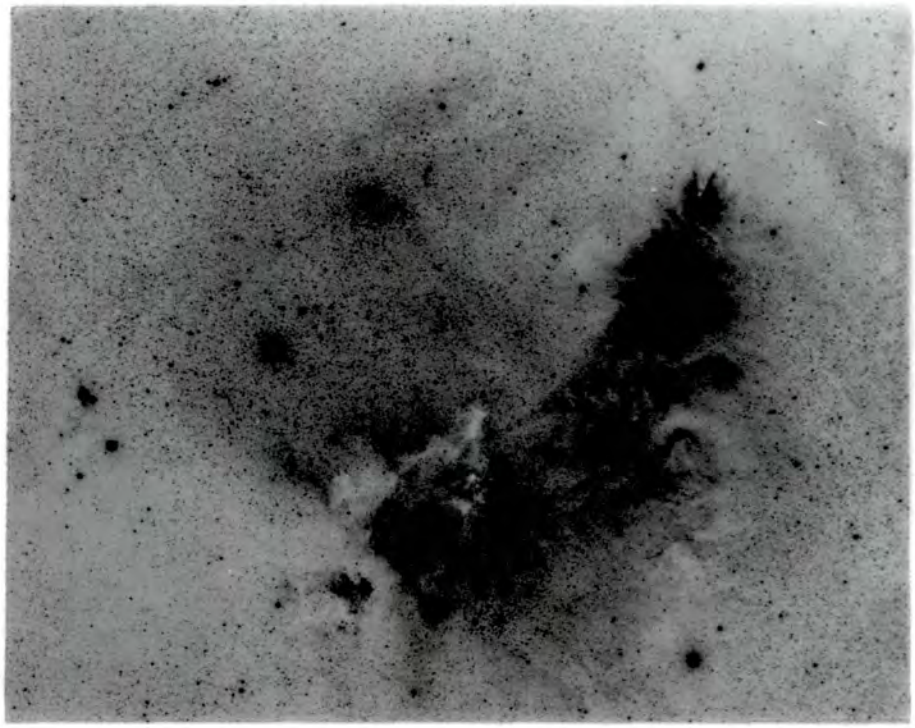

Fig. 4.1

**Photographs of the Cone(IRN) 1 and 2**

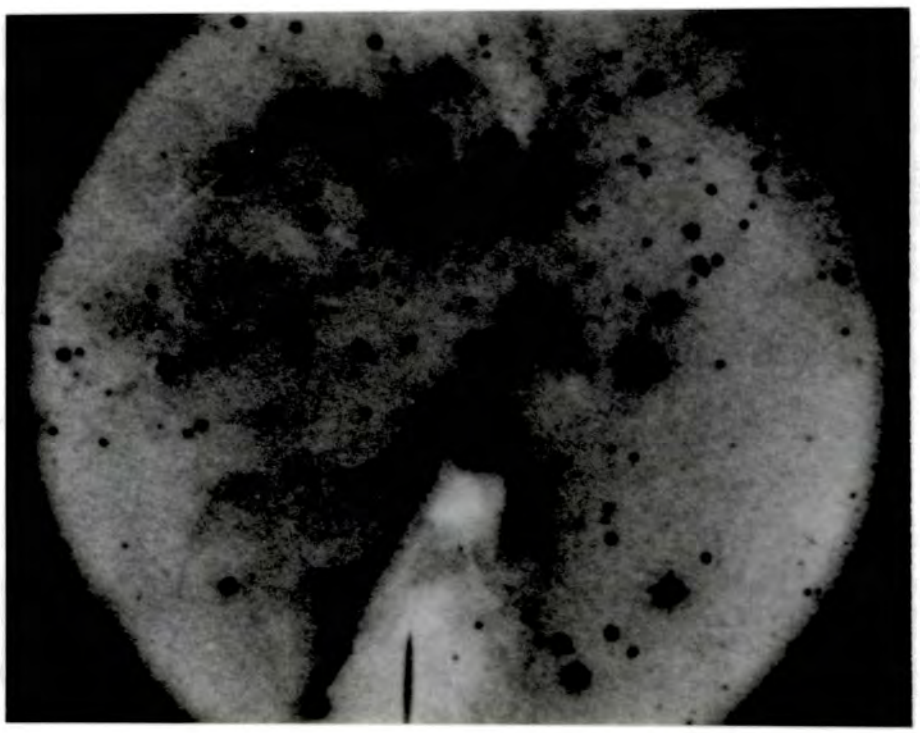

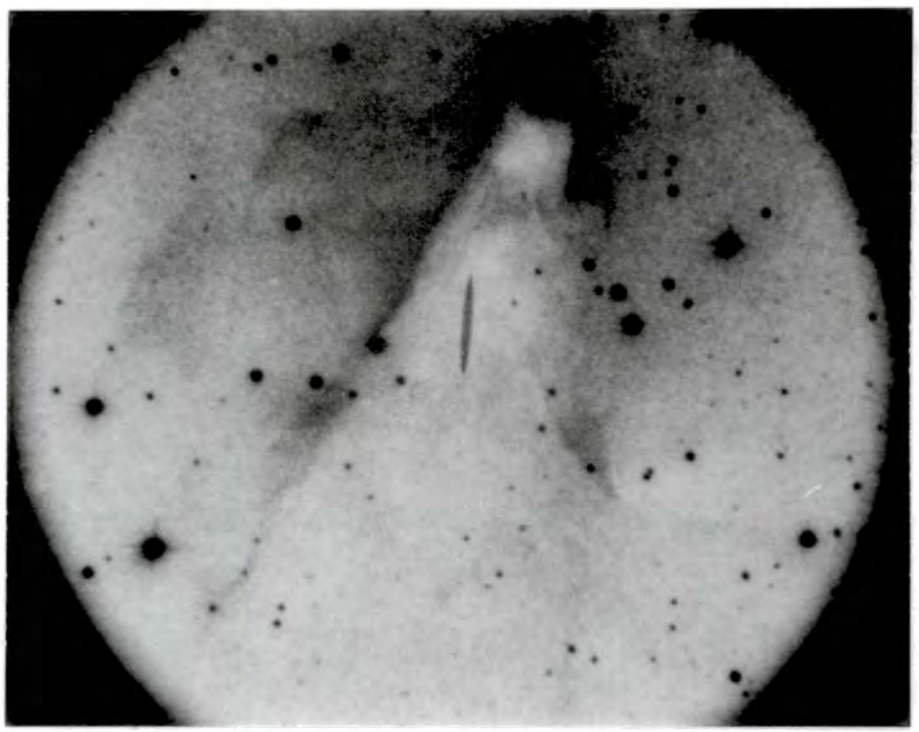

Fig. 4.2

**Photographs of the Cone(IRN) 3 and 4**

NGC2264 but as yet uncondensed into stars. Crutcher, Hartkopf and Giguere (1978) found that theNGC2264 molecular complex consists of at least six distinct clouds with a total mass of approximately 2 x $10^4$ $M_{0,}$ while the mass of the recognised stellar population is only about 20 percent of this value, and so the region is of particular interest in the study of star formation.

NGC 2264 has been used as a "testing ground" for many areas of study, particularly in trying to understand the process of star formation. T Tauri stars and YY Orionis type variables have been found in the cluster, the latter type are very young, with ages of approximately 3x$10^4$ to $10^6$ years, and masses of 0.5 to 2 times the mass of the sun. It is believed they have only recently appeared from their accretion envelopes, and are the youngest stars optically visible in the cluster, (Walker 1972). The large number of T Tauri stars in the region could suggest that cloud formation has been an important source of low mass stars, and the presence of larger O and B type stars may have helped to dissipate the cloud fragments.

The Cone appears to be associated with an elongated foreground "Bok Globule" which has bright, ionised edges. (Schmidt 1974). The visual features of the cone are apparently located in front of a molecular cloud which extends to the north-west. The denser part of this cloud has been mapped in $CH_2$ O absorption (Rickard et al. 1977), and CO (Crutcher et al, 1978). From their results they found the cloud to be elliptical in shape, consisting of two condensations, (Blitz 1978)

The Bok globule is situated near the cone, to the south of the HII region. In 1972, Zuckerman et al. searched for millimetre wavelength molecular lines and although their search was successful, they did not think that the source was associated with the globule, but rather with the background cloud. In 1976, Rickard, Palmer, Buhl and Zuckerman observed 6 cm formaldehyde absorption over an extended region surrounding the globule in NGC 2264.

Walsh (1980) published a detailed classification of data for NGC 2264, in optical, infrared and radio wavelengths. By this time, eleven molecular species had been observed in NGC 2264, with peak molecular emission and absorption occurring just south of Allen's Infrared object, (GL989), and very

near to the ConeIRN. In his discussion, Walsh proposed that the NGC 2264 cluster and the optically visible HII region appeared to be situated in front of the molecular clouds. By comparing the radial velocity of the ionised material and the cluster, with that of the molecular clouds, it shows that the HII region has a similar, or slightly greater velocity of recession, (i.e. approaching the clouds).

Many of the less luminous pre-main sequence A - F stars still seem to be surrounded by circumstellar gas or dust, and there is a correlation between circumstellar shells and variability, (Breger 1972). The brighter stars which have thinner shells, do not display a marked variability. The gas envelopes consist of hot ionised gas, with temperatures of about $10^4$ K. The more luminous stars have, however, "blown off" the smaller dust particles by radiation pressure, and the larger dust particles which have remained could be an explanation for the "grey" optical absorption at visual wavelengths.

Allen's Infrared object (GL989) was discovered in 1972 when Allen carried out a survey of IR objects in HII regions. He searched the central region of NGC 2264 and found an IR source which did not correspond to a visible star. This source lies close to the apex of the cone nebula, and its 1950 co-ordinates are;

$$\alpha = 06^h\ 38^m\ 24^s$$
$$\delta = 09\ 32\ 29$$

As NGC 2264 is a relatively young cluster, and many of its stars are enveloped in dust shells, which are detectable at IR wavelengths, Allen proposed that at the apex of the cone, there was probably a normal star heavily obscured by dust.

Allen used a distance modulus of 9.2 and deduced a minimum luminosity of 1000 $L_o$ which would mean that it would be one of the most luminous objects in the cluster. However, Allen stressed that because of the rise at 2.2 microns it was difficult to assess the total luminosity of the system. It was also noted that the IR source lies not only at the apex of the small nebula but also at

the projected apex of the linear segments of the more well-known cone nebula. Such a position in NGC 2264 would favour the interpretation that the IR source is the most massive and luminous object in the cluster. The luminosity has a maximum value of 3500 $L_o$ which peaks at approximately 200 microns, so is presumed to be heavily obscured since it has never been observed in visible wavelengths. An upper limit of m>19 at around 9000 angstroms was found by Allen.

The long wavelength spectral distribution suggested to Harvey et al. (1977) that not a single black body is observed, but rather a number of such, each with a different temperature arranged in such a way that a temperature gradient is observed. Measurements of the IR source at near IR wavelengths show that GL989 is smaller than 0.2", which corresponds to 160 A.U. at a distance of 800 parsecs, (the distance calculated by Adams, Strom and Strom.) Brackett line emission from GL989 was discovered by Thompson and Tokunaga in 1978. The ratio of $B_\alpha$ /B $\gamma$ was measured by Simon et al, (79) and found to be 3.5 ± 0.5, where B$\alpha$ is the first, and B$\gamma$ is the third line in the Brackett series. This data was found as a result of a B$\alpha$ line survey of compact Infra-red sources, believed to be in the early stages of star formation. They detected B$\alpha$ from four cometary nebulae, one of which was NGC 2264.

Molecular features observed in the vicinity of GL989 include a $H_2O$ maser (Genzel and Downes,1977) and molecular species such as CO, OH, $NH_3$, CS.

## 1.2) Cone IR Nebula (Cone IRN)

This feature is adjacent to GL989 (Allen's Infrared object), and is the small fan-shaped nebula which is of interest in this study. Schmidt referred to this small "knot of nebulosity" in his paper in 1972. Following Allen's results, optical observations were made of this object to determine its nature. Schmidt found the object to be of particular interest, and to determine its association with the infrared source. Although the "knot" appears to be embedded in a HII region, its spectrum is continuous with no line emission. Schmidt also investigated the total flux of the knot and the energy distribution at visual wavelengths. His results suggested that the nebulosity could be a reflection nebula. If the "knot"

is a dense cloud illuminated by a star within it, then the energy distribution of the knot as a whole will resemble that of a star, providing that the geometry of the nebula is not such that it would allow the light to escape preferentially in one direction. After further specific investigation, Schmidt also found a hint of Hα emission detected near the apex of the "knot".

## 2) INTERPRETATIONS

Schwartz et al (1985), believe that Allen's IR source (GL989) is an early type star, probably about B3 V, which is embedded in a dense molecular cloud. The heat from the source ionises a small HII region. The Star is very young and drives a molecular flow, (broad winged CO emission supports this.) The star has apparently formed from, and is still embedded in a portion of a high density rotating molecular ring, seen nearly edge on. This ring is quasi-stable against rapid radial collapse, but may be in the process of being flattened into a disk. They also believe that other young stars, probably of lower luminosity may have formed in the northern part of the ring. The ring is rotating in such a way that it appears that the IR source is receding.( See figure 4.3 overleaf.)

The mass of such a 'doughnut-shaped' cloud, which would produce the observed molecular maps, would have to be about 750 times greater than the mass of the sun, and it is believed that the cloud may be near to equilibrium or about to collapse. The redshift of the gas at positions of highest projected density may be interpreted as radial inflow of the ring, perpendicular to the direction of rotation, i.e. the ring is collapsing to a disk with a central hole.

Brosch and Greenberg (1985), however, believe that the cone is generated through the interaction of a channelled wind from Allen's IR source (GL989) and the Bok globule. The north-ward emerging wind affects the cloud through momentum transfer to create the Herbig-Haro objects. The wind may be "observed" as the small (apparent) reflection nebula (ConeIRN), which reflects light from the IR source. The southward wind shapes the Cone nebula by leaving an unaffected region in the shadow of the Bok globule. The surface of the wind on the globule is visible as the enhanced emission region. The spectral characteristics appear to indicate shock ionisation rather than

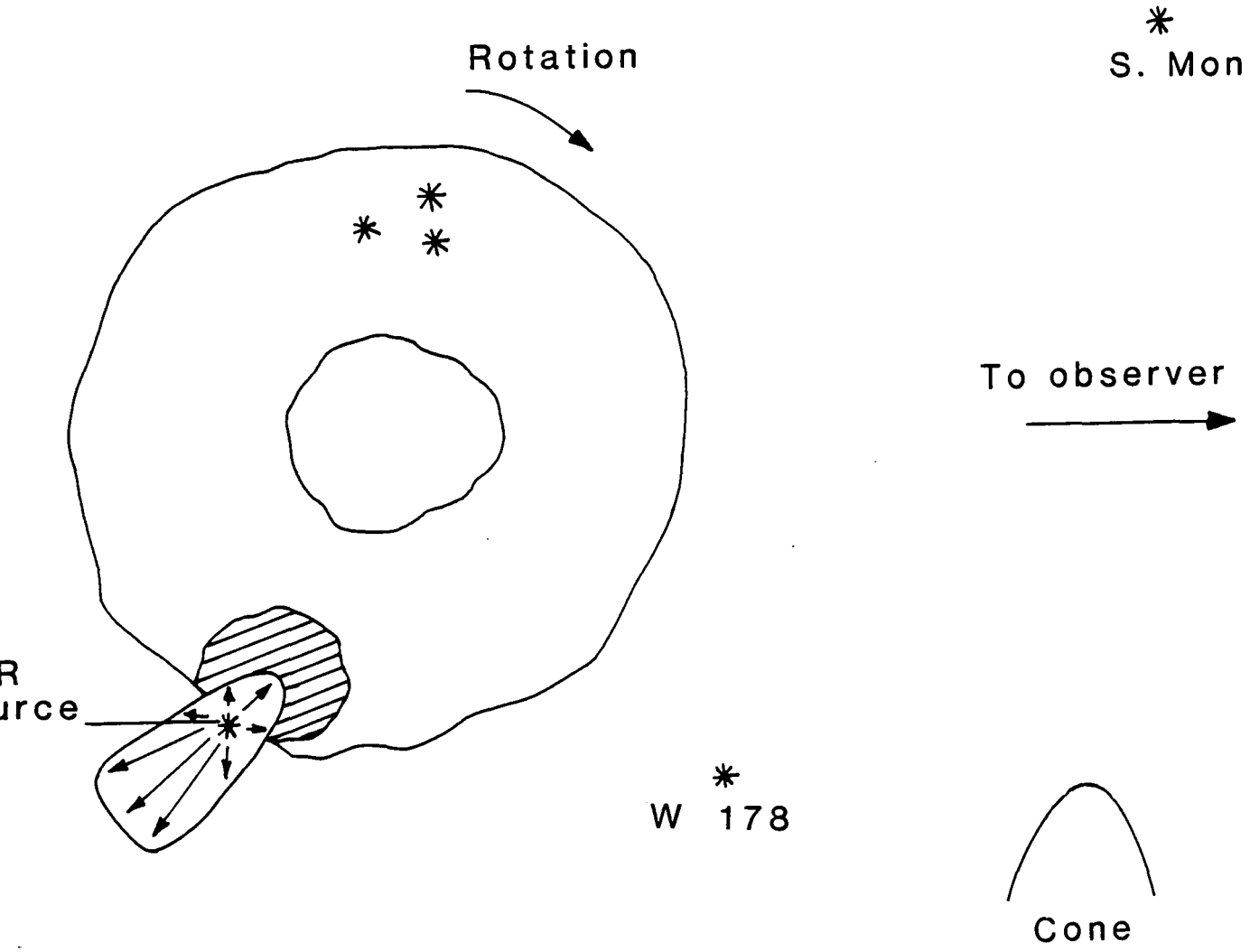


Fig. 4.3

Rotating ring model (Schwartz).

radiative ionisation. The model agrees well with the molecular cloud dynamics. (See figure 4.4)

Harvey et al. proposed a model in 1977 which involved dust clouds, such that dust at varying temperatures is viewed through a "hole" in the surrounding dust clouds, whilst the stellar source is obscured behind a denser cloud. This model attempts to explain the presence of the nebulous knot (cone IRN) and the IR source (GL989), for which a unique black body temperature is not sufficient. It is believed to be more than a coincidence that the infrared object lies at the projected apex of the Cone nebula.

Walsh (1980) believes that the Cone(IRN) cannot be a reflection nebula produced directly by an existing star, unless that star is very red. If it was a reflection nebula changes in brightness would be expected as the dust shell about the IR source fragments. (See figure 4.5 overleaf.)

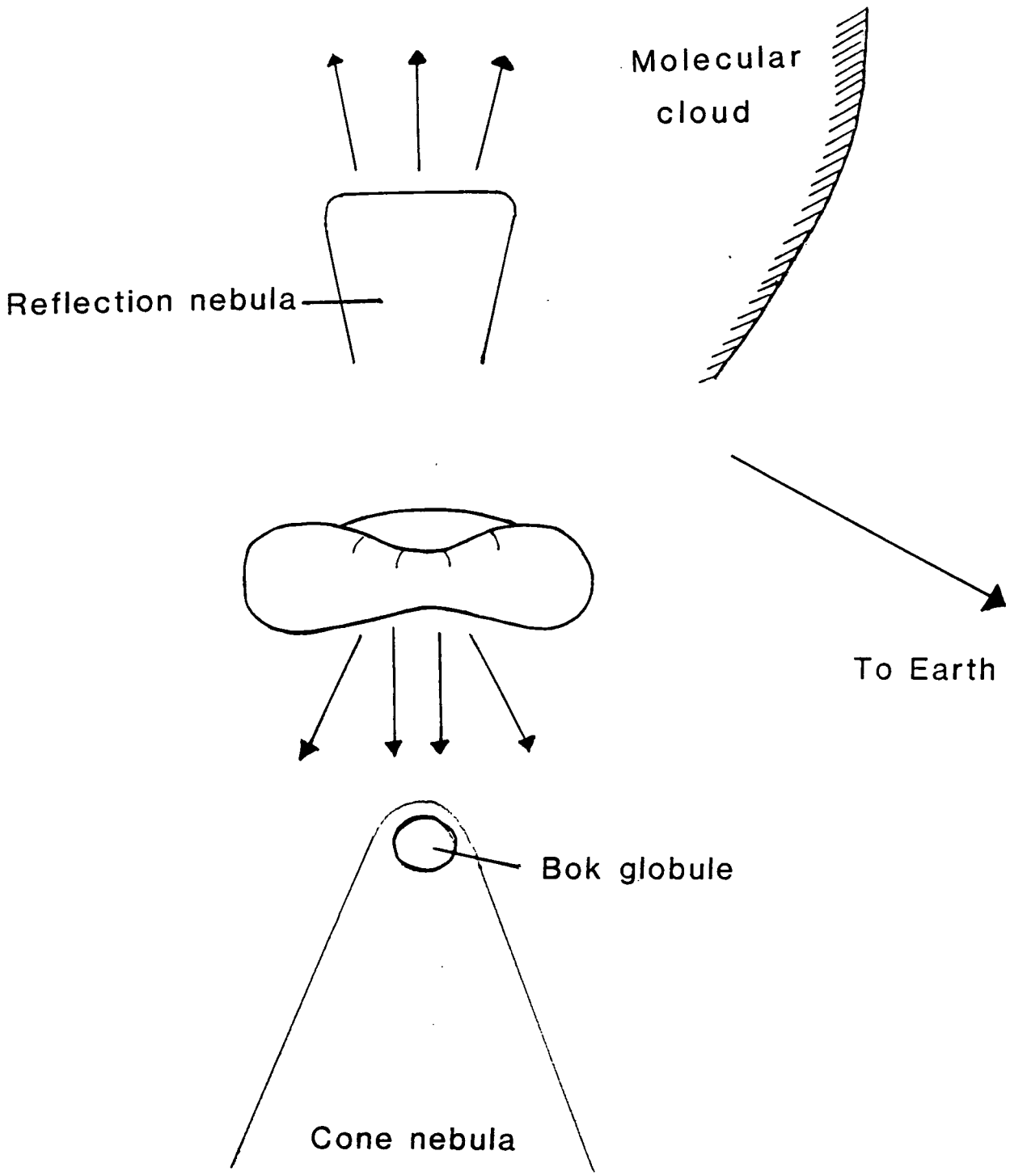


Fig. 4.4 Brosch and Greenberg model.

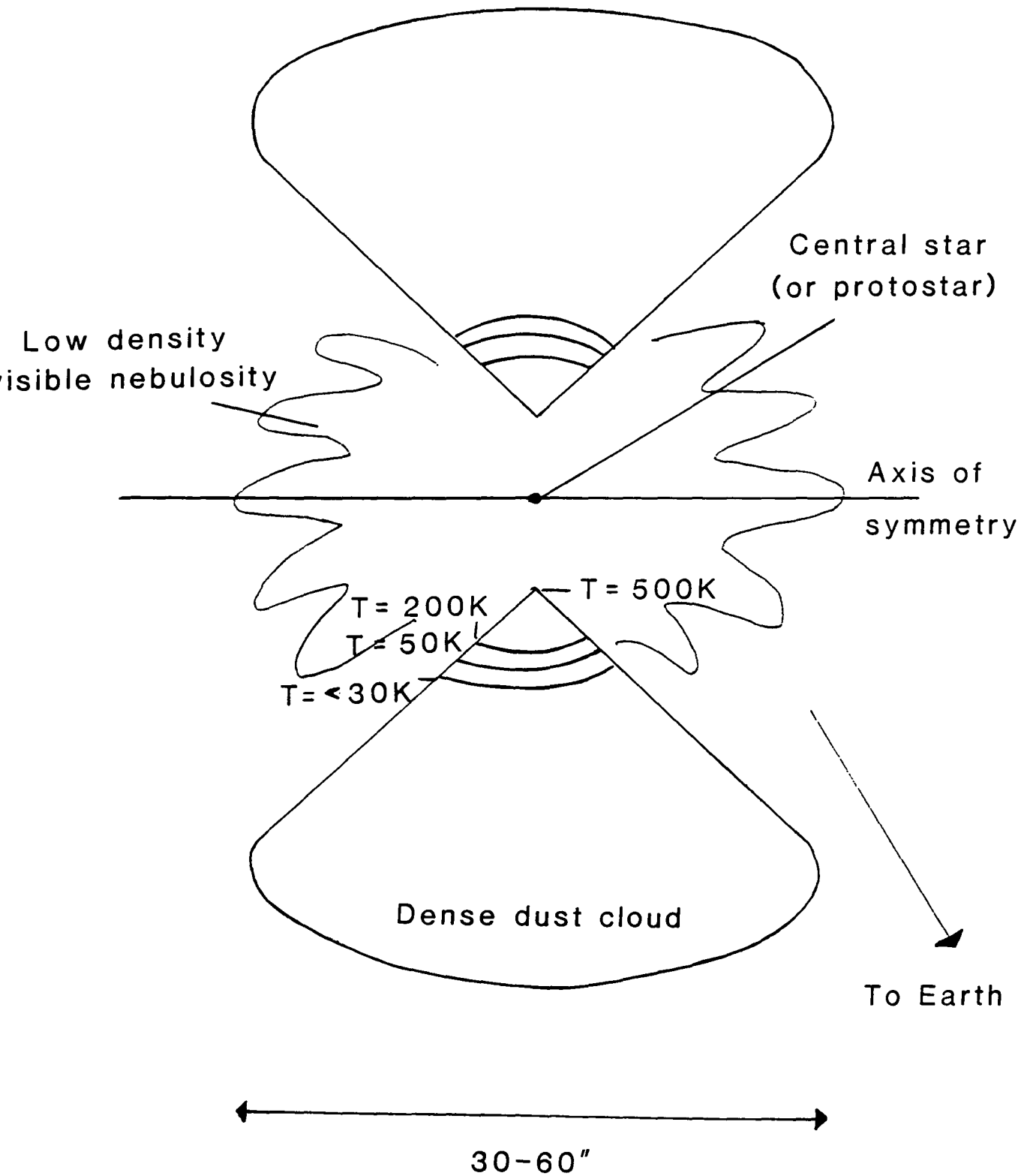


Fig. 4.5 Harvey's model.

# CHAPTER FIVE
# THE POLARISATION DATA

The observations were made at the 1 metre telescope at the Wise Observatory, Israel, during February 1985, using the Durham Imaging Polarimeter and using a CCD detector system based on the GEC P8600 chip (Wright and Mackay, 1981). The data was reduced at the Durham University node of Starlink using DIPS/EDRS programs, written mainly by R.F. Warren-Smith.

## 1) THE DURHAM POLARIMETER

The design of the polarimeter was based upon the suggestions of Pickering (1873) and Ohman (1939). They proposed that a plane parallel slab of calcite could be used to separate polarised images, by a series of parallel obscuring strips inserted into the focal plane of the telescope, which they referred to as the "grid". The lens system produces an image of this, using a Wollaston prism. The prism produces two images and each exposure then appears to be a series of paired strips. Figure 5.1 shows the construction of the polarimeter.

In order to produce a polarisation map, four exposures are made, with the plane of polarisation of the incident light rotated through 45 degree intervals. An achromatic half wave plate in front of the prism is used, and the procedure is described in detail by Apenzeller (1967), and Serkowski (1974). By using

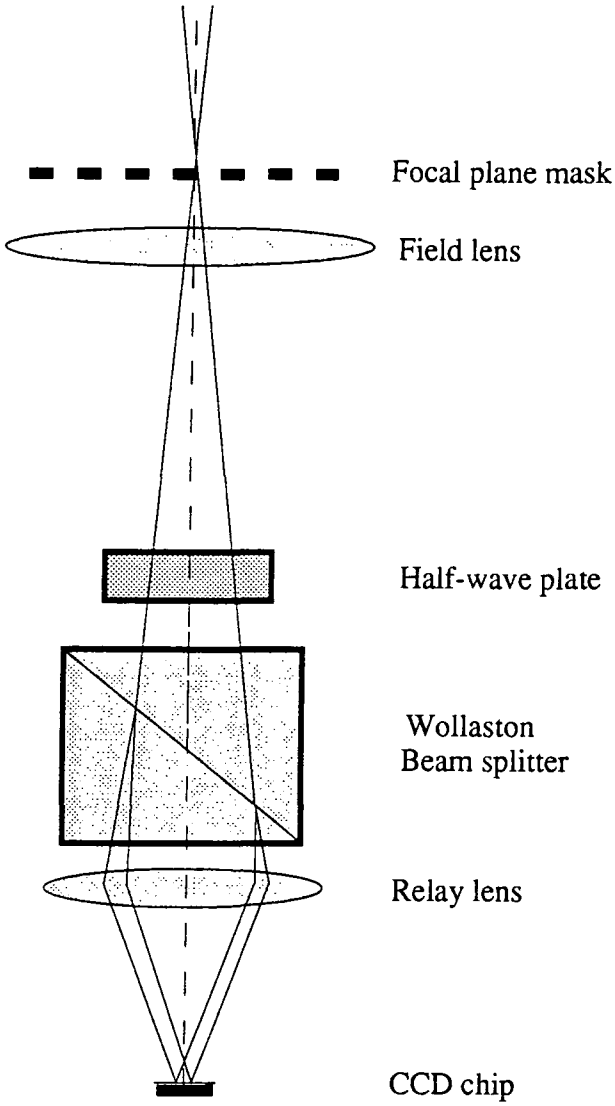


**Fig. 5.1**

**The Durham Polarimeter**

half wave plates, it enables the observations to be more thorough. The grid spacing is small, to avoid chromatic dispersion in the prism, and set at 3.15mm in the focal plane of the telescope.

The Wollaston prism produces the two orthogonally polarised images, with an angular divergence of one degree between the two emerging polarised rays. The small angular divergence avoids the effects of chromatic dispersion, which could result in elongated images of the stars. See figure 5.2 to show the view in the plane of the telescope, and the focal plane view when re-imaged through the beam splitter and then recorded on the CCD.

When observing an astronomical object, a series of four exposures are taken corresponding to the four half wave plate positions, then the process is repeated with the grid moved to its second position to observe the second half of the field. However, exposures must be taken to observe the flat field response of the CCD, and this is done by observing a uniformly illuminated screen on the inside of the observatory dome. The background night sky signal needs to be taken into account, and this is achieved by selecting appropriate image regions to then estimate and subtract from the final data.

## 2) CCD POLARIMETRY

The Durham imaging polarimeter was used to obtain the polarisation maps. It was used extensively between 1974 and 1982, with an electronographic camera as a detector, and has been described by Warren-Smith (1979), and Scarrott et al. (1983).

The electronographic camera proved useful, but it had several problems associated with the processing of the plates, and developing the data. A new detector system was needed which could produce higher quality data, and with greater light sensitivity. The charged coupled device (CCD) camera system became increasingly more popular. The advantages of the CCD system over the previous methods were that, first of all, it was easier to use practically, but also with this system, the images were available for inspection as soon as the exposure was taken. The response of the CCD system to light intensity is linear, which was not the case with the former electronographic

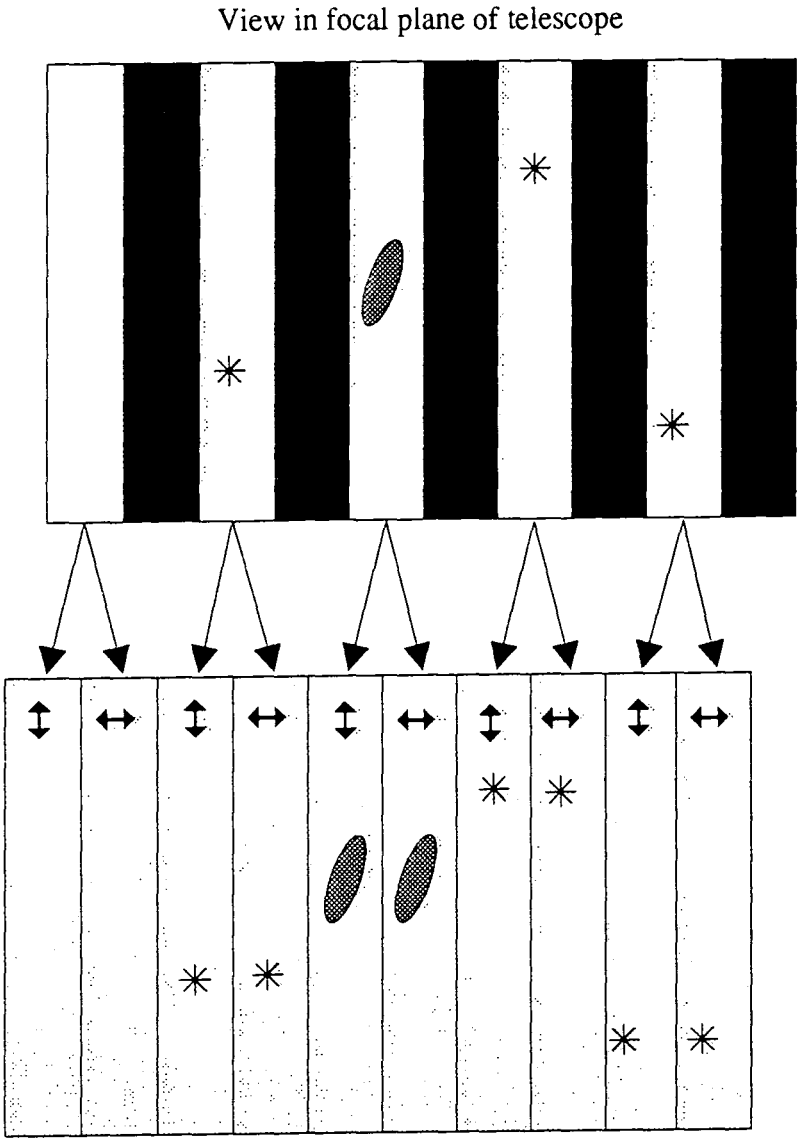


**Fig. 5.2**

**Polarimeter Images**

camera.

The most sensitive type of CCD are machined thin to allow blue photon penetration and detection in the CCD substrate. However, a problem which may occur is "fringing", which is due to emission lines reflecting and interfering within the very thin substrate, and cause effects similar to thin films and Newtons rings. As the CCD surface cannot be machined to sufficient accuracy, which would be less than one wavelength, the fringing would have significant affects upon the data. To avoid such problems and minimise errors, it was then decided to use instead, an unmachined thick CCD.

Thick CCDs have no fringing problems, but have little sensitivity in the blue end of the spectrum, and none at all in the ultra-violet. This is a great disadvantage since most reflection nebulae are identified by their intrinsic blueness, and are more luminous at these wavelengths. The CCDs respond well into the infrared, to about one micron, which extended beyond the limits of the electronographic camera, and so this opened up the possibility of extending polarimetry studies further.

The CCD system was designed and built by Craig Mackay from Cambridge University. The original system used a GEC MA357 CCD detector (Wright and Mackay, 1981). The Durham CCD was built in 1984 and uses a GEC P8603 detector. The introduction of CCD detectors improved the opportunity for efficient observations of nebulae, with the advantage of allowing the recording of an entire nebula, including the surrounding sky, in a single exposure. Other advantages included high quantum efficiency, high photometric accuracy, and a wider range of spectral sensitivity.

Originally, the control computer was a Data General Nova 4/C, which was a 16 bit general purpose mini computer with a memory of 64k. Image display was achieved using an image store, which can display images on a black and white monitor. These images can be up to 640 x 512 pixels, with each pixel consisting of up to 12 bits of information. The system also has a magnetic tape unit, which is a streamer device which can read and write to a 9 track computer tape for general data transport. Figure 5.3 shows the current situation, where the Durham imaging Polarimeter is connected to the control room, which has

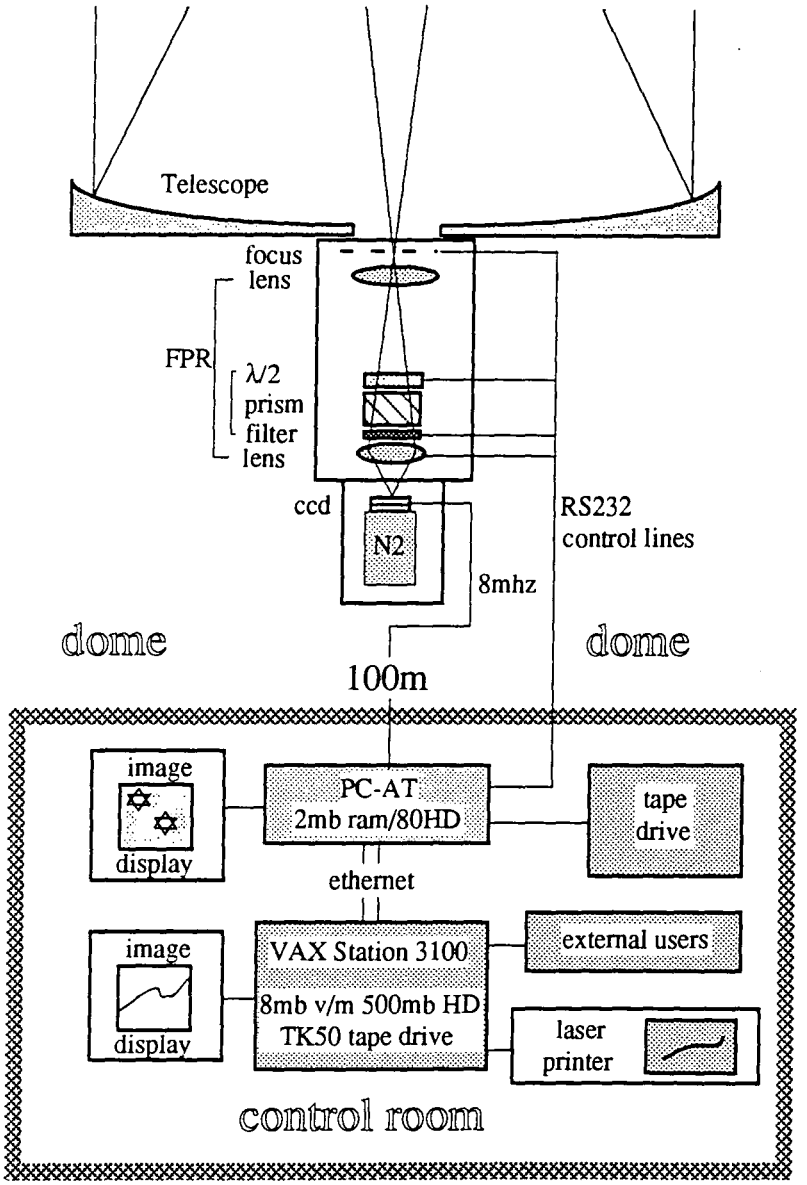


**Fig 5.3**

**Durham Imaging Polarimeter**

been the system used since 1990.

The CCD frames are stored in a Flexible Image Transport System format (FITS) (Wells, Greisen and Harten 1981) which can be read on most computers. On line data storage is performed on a winchester hard disk which can store up to 70 megabytes of information, which corresponds to about 70 CCD frames.

The CCD, as mentioned earlier, is a GEC P8603/B analogue integrated circuit, consisting of 576 x 385 picture elements ( pixels ), which are sensitive to light. Each pixel is 22 microns square, and act as metal oxide semiconductor (MOS) capacitors, forming a potential well into which the charge carriers ( electrons or holes ) can accumulate. The energy band gap is such that the energy from one single photon is enough to free a charge carrier, therefore one detected photon corresponds to one released charge carrier.

At the end of the exposure time, the shutter is closed to prevent further activation of the CCD, and the frame is "read out", which is a process controlled by the host computer. The electronics rack transmits the potentials necessary to cause the charge to transfer to the output registers, and then it can be amplified and converted to a digital form.

The CCD is ideally kept at 120K to reduce the "dark current", i.e. electrons can gain energy from thermal excitations and be released into the conduction band. Other sources of noise are the shot noise of the photons themselves, the readout noise, and the noise from the electronics rack. Noise and bad data which have to be considered also are cosmic rays, hot spots, dead pixels, bad columns, charge transfer inefficiencies and also charge overflow and smearing.

Generally, exposure times used are short enough to avoid the build up of cosmic rays, and can be ignored for exposures of short duration. In fact, exposures of up to twenty minutes are possible before the effect of cosmic rays become apparent. If an object requires longer exposure times, then multiple exposures are taken as opposed to one long exposure, to avoid the effects of cosmic rays.

When the CCD data has been taken and written onto the tape, it must then

be converted on the Durham node of Starlink into a standard format, before it can be analysed to produce the final polarisation maps and intensity images, using the Durham Imaging Polarimetry system (DIPS) programs, developed by Dr. R.F. Warren-Smith. The preprocessing programs were produced by R.F. Warren-Smith and P.W. Draper.

## 3) THE POLARISATION DATA

Observations were made in the four wavebands, V,R,I and Z, details of which are given below. The observations were made during February 1985 at the Wise Observatory in Israel.

Table 1 gives information with regards to the observations.

TABLE 1

| Filter | Wavelength (nm) | Number of images | Exposure time(mins) | Total exposure time (mins) |
|---|---|---|---|---|
| V | 555 | 4 | 10 | 40 |
| R | 669 | 12 | 2 | 24 |
| I | 784 | 7 | 4 | 28 |
| Z | 932 | 4 | 10 | 40 |

Table 2 shows the Full width, half maximum (FWHM) values for the various filters.

TABLE 2

| wavelength (nm) | bandwidth |
|---|---|
| 555.523 | 45.072 |
| 668.868 | 86.082 |
| 783.819 | 62.848 |

A major source of error in the study of polarimetry, is the problem of taking into account the background signal of the sky. This background signal needs to calculated and subtracted from the data to be reduced. It is found by selecting some area of the sky, in the vicinity of the area to be studied, which gives a good representation of the sky background which is unaffected by the object itself. It is possible to locate areas of low intensity, within the field of view of the object, and use these regions to calculate the background sky signal. This method has many advantages over previous methods employed by polarimetrists, as it does not waste valuable observing time, gives a wider choice of sky regions to select after the observations have been made, and leads to a consistency in the calculations of sky subtraction.

## 3.1) The polarisation maps

Figures 5.4, 5.5, and 5.6 show the polarisation maps with the V, R and I filters respectively. The right hand side maps show the light intensity contours. For clarity, the maps have a lower level of intensity cut-off, ( minimum intensity of 100 ), which reduces contamination of the results by low intensity vectors, which are of a random nature, and not really indicating the underlying pattern of the nebulosity.

The polarisation maps indicate the distribution of linear polarisation at various positions in the nebula. The polarisation at a point is represented by a line, the length of which is proportional to the percentage polarisation at that point, parallel to the E-vector. The integration bins for the maps are 3 x 3 arcsecs, with 1.2 arcsec per pixel.

Figure 5.4 shows the polarisation distribution using the V filter (555 nm.), and the light intensity contours show the arcuate structure of the nebulosity.

The co-ordinate system used for the polarisation and light intensity maps has been in such a way that the bright centre of the luminosity is at the position (0,0), which is consistent with the approach adopted by Brosch and Greenberg, (1985).

Using this co-ordinate system, then Allen's Infrared object (GL989) would

be located at approximately - 10 R.A., 0 Dec according to our coordinate system. However, from the maps produced, there is no obvious sign of its presence at optical wavelengths.

Figure 5.5 shows the results with the R filter (669 nm.), and the distribution of the polarisation vectors is much more distinct, showing a pattern of alignment.

Figure 5.6 shows the results with the I filter (784 nm), again showing the pattern of alignment of the polarisation vectors.

## 3.2) Wavelength dependence of polarisation

The following table gives the polarisation values at various positions;

TABLE 3

| position | V | R | I | Z |
|---|---|---|---|---|
| 0,0 | 3.9 ± 1.1 | 5.1 ± 0.6 | 4.9 ± 0.6 | 0.8 ± 2.8 |
| 5,-5 | 6.8 ± 1.9 | 9.1 ± 1.0 | 12.2 ± 1.2 | 5.4 ± 5.1 |
| 10,-10 | 3.3 ± 2.5 | 7.7 ± 1.5 | 7.6 ± 2.0 | 21.5 ± 9.7 |
| 10,5 | 6.1 ± 1.5 | 5.5 ± 0.8 | 4.7 ± 1.0 | 8.08 ± 5.9 |
| -5,5 | 3.7 ± 3.0 | 4.7 ± 2.1 | 10.5 ± 2.9 | 14.8 ± 8.5 |
| -5-5 | 3.0 ± 2.5 | 4.1 ± 1.6 | 6.3 ± 1.4 | 7.2 ± 3.3 |

Figures 5.7 to 5.12 show the variation of percentage polarisation with respect to wavelength for various positions over the nebulosity.

Figure 5.7 shows how the percentage polarisation varies for the bright centre of the nebulosity, at the coordinates (0,0) on the polarisation maps. At this point, the polarisation is higher over the R,I wavelengths.

The other figures correspond to various positions located about the bright centre of the nebulosity, at the co-ordinates.

TABLE 4

| figure | co-ordinates |
|---|---|
| 5.7 | (0,0) |
| 5.8 | (5,-5) |
| 5.9 | (10,-10) |
| 5.10 | (10,5) |
| 5.11 | (-5,5) |
| 5.12 | (-5,-5) |

The figures 5.7, 5.8, 5.9 are showing the wavelength dependence of the polarisation at positions of increasing distance from the bright centre outwards, and indicates how the polarisation varies with position and wavelength. As the distance from the bright centre increases, the accuracy of the data decreases, but the variation of the percentage polarisation can be seen to fluctuate.

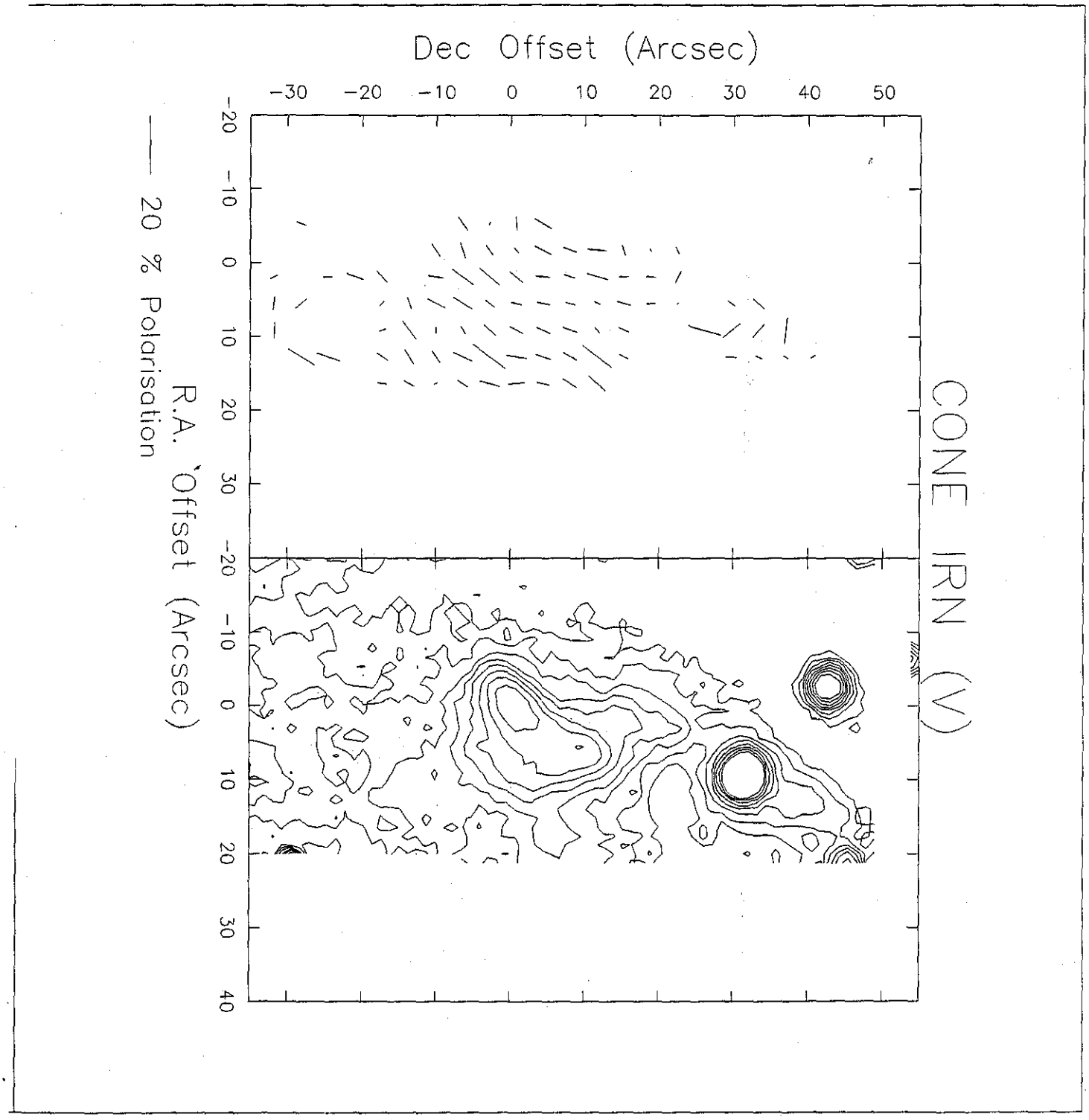
Dec Offset (Arcsec)
−30 −20 −10 0 10 20 30 40 50
−20 −10 0 10 20 30 −20 −10 0 10 20 30 40
R.A. Offset (Arcsec)
20 % Polarisation
CONE IRN (V)

Fig. 5.4

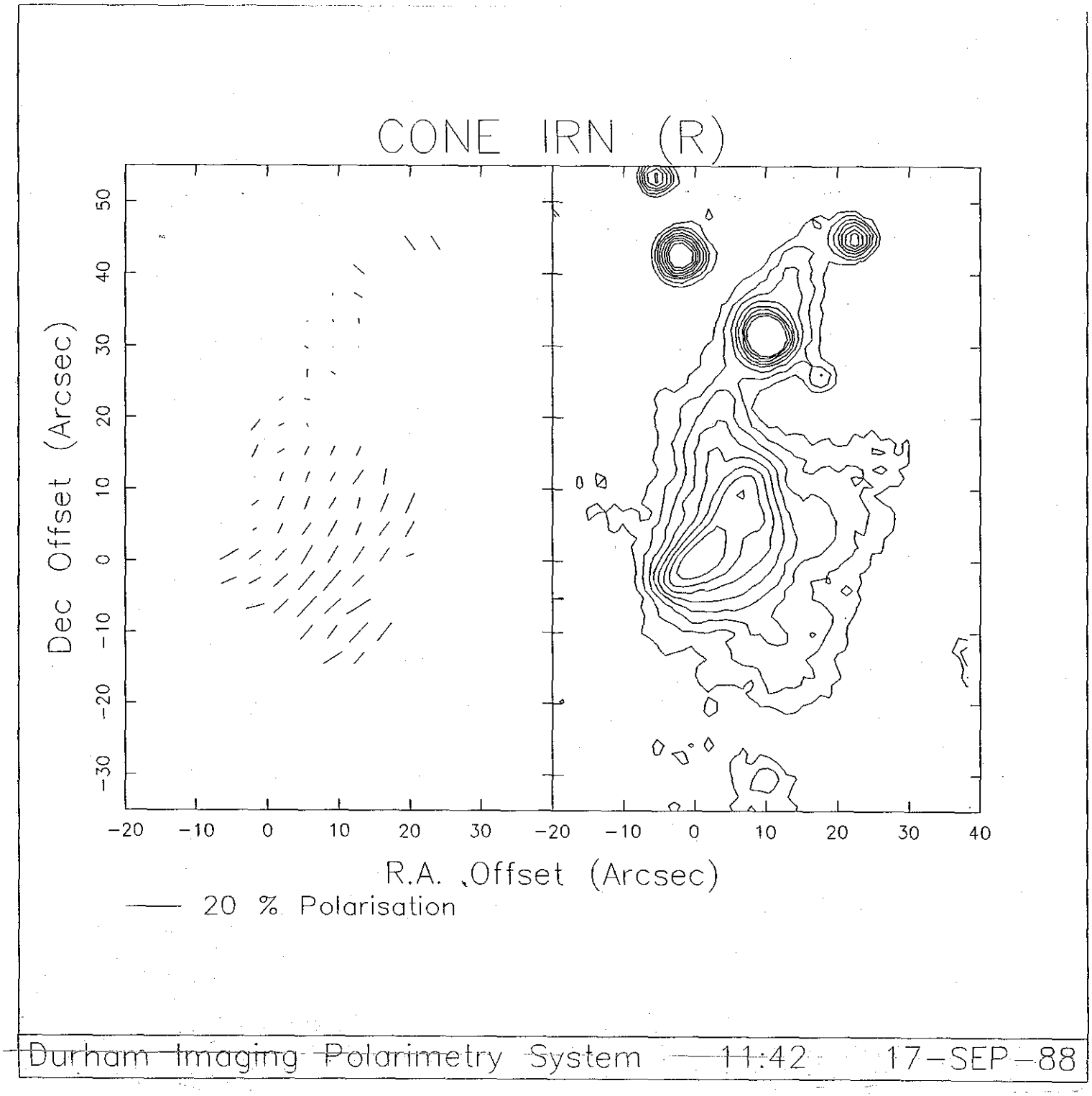
CONE IRN (R)
Dec Offset (Arcsec)
50
40
30
20
10
0
-10
-20
-30
-20
-10
0
10
20
30
-20
-10
0
10
20
30
40
R.A. Offset (Arcsec)
20 % Polarisation
Durham Imaging Polarimetry System
11:42
17-SEP-88

Fig. 5.5

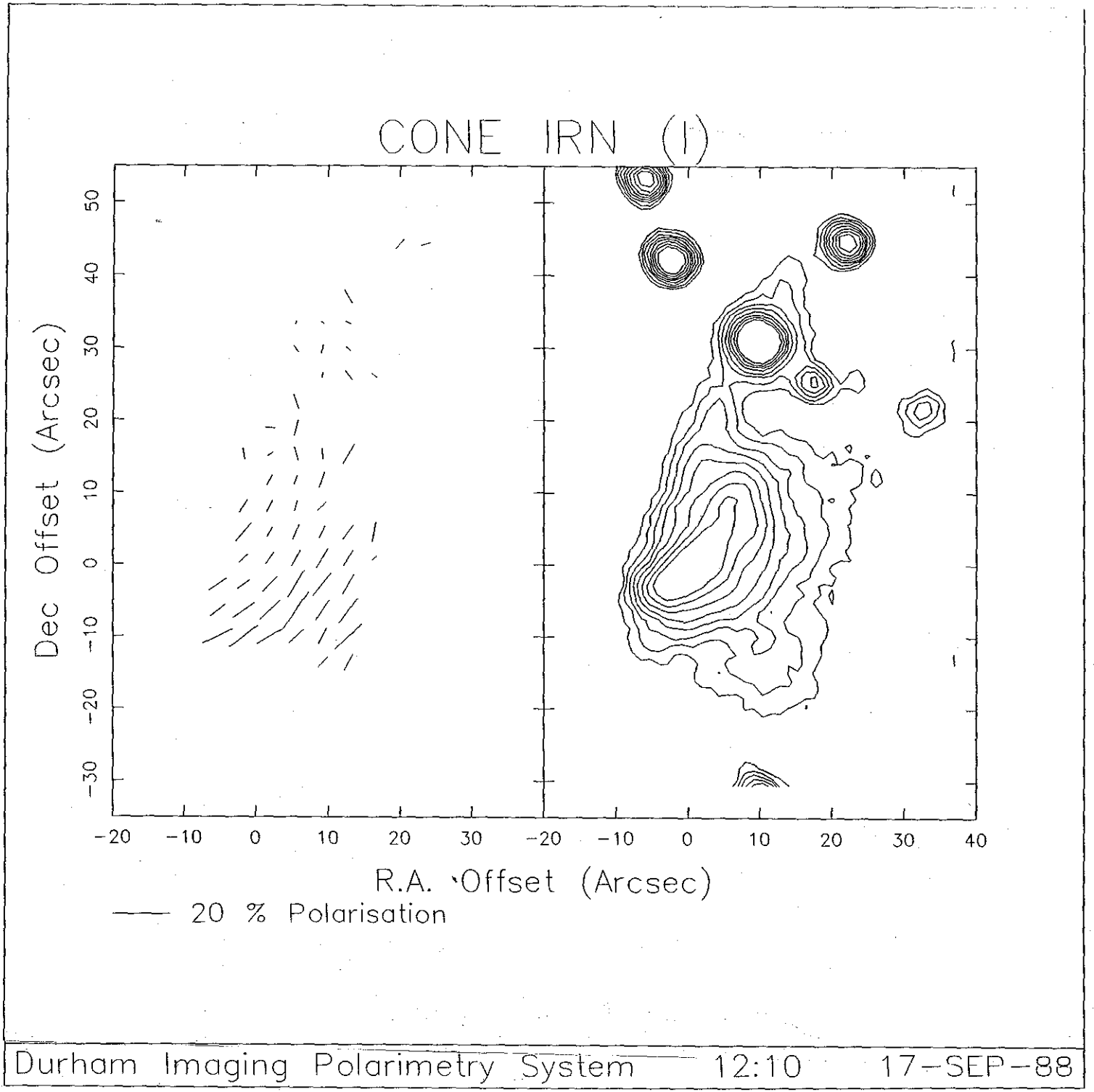
CONE IRN (I)
Dec Offset (Arcsec)
50
40
30
20
10
0
-10
-20
-30
-20
-10
0
10
20
30
-20
-10
0
10
20
30
40
R.A. Offset (Arcsec)
20 % Polarisation
Durham Imaging Polarimetry System
12:10
17-SEP-88

Fig. 5.6

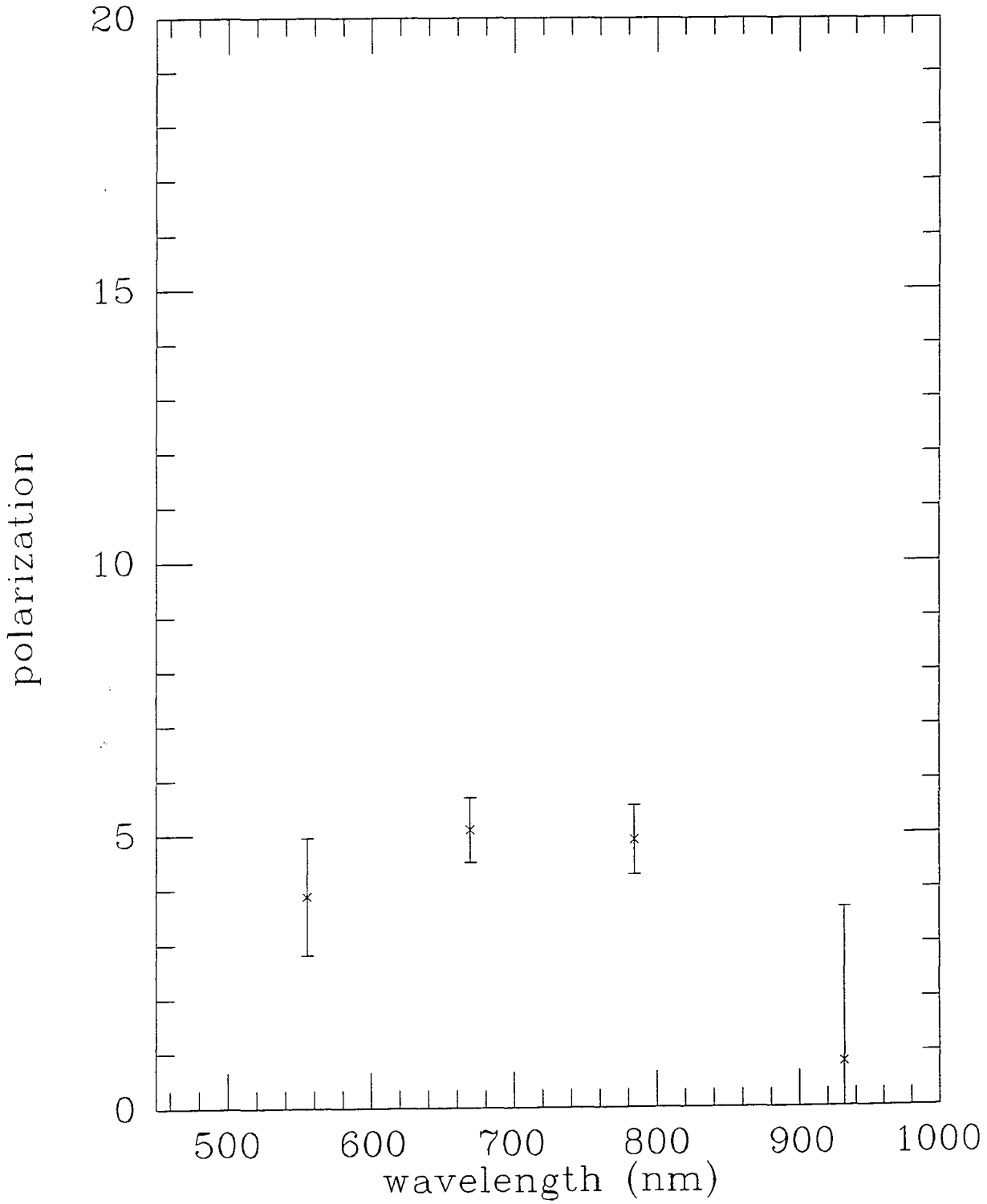
20
15
10
5
0
polarization
500
600
700
800
900
1000
wavelength (nm)

Fig. 5.7

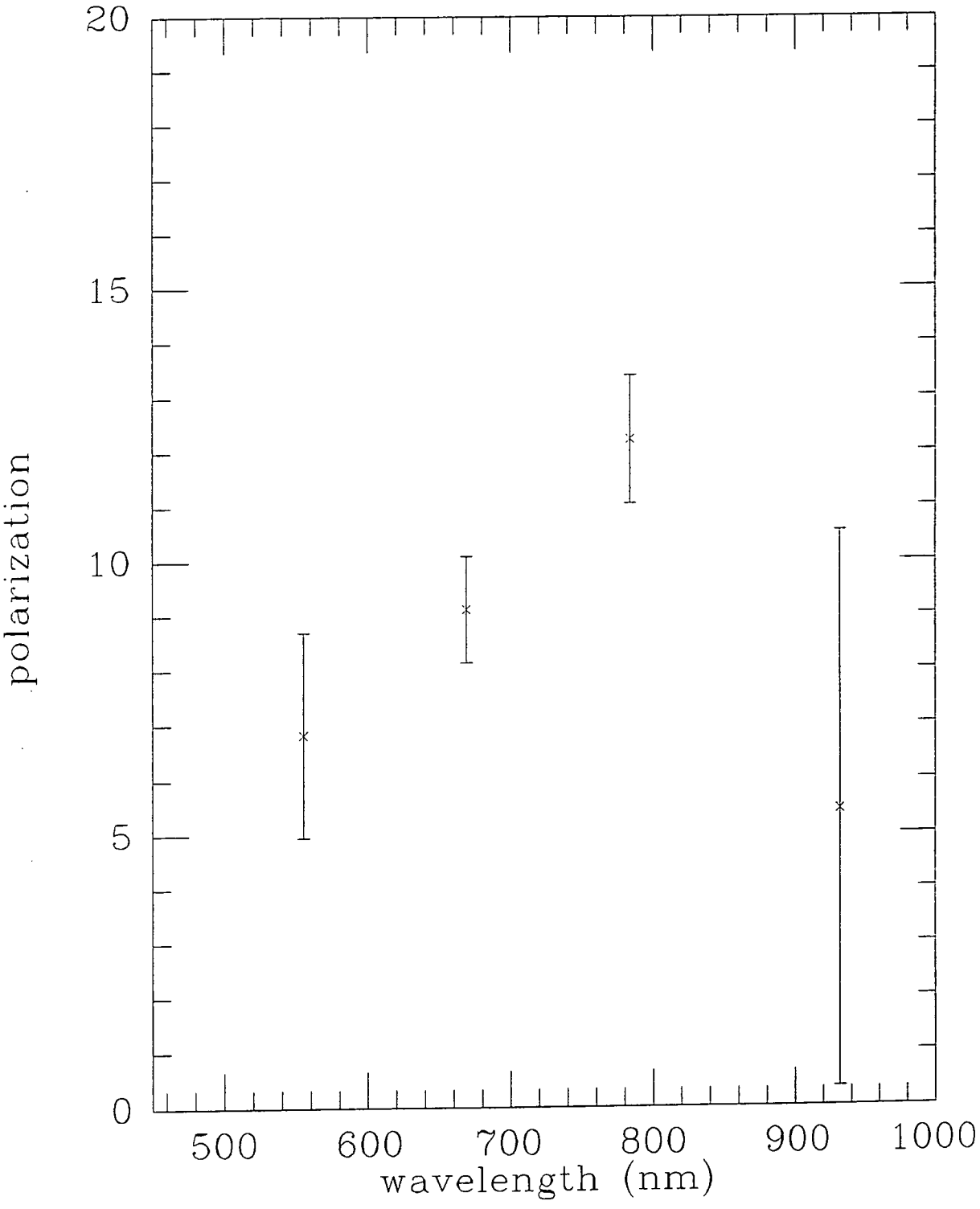
20
15
10
5
0
polarization
500
600
700
800
900
1000
wavelength (nm)

Fig. 5.8

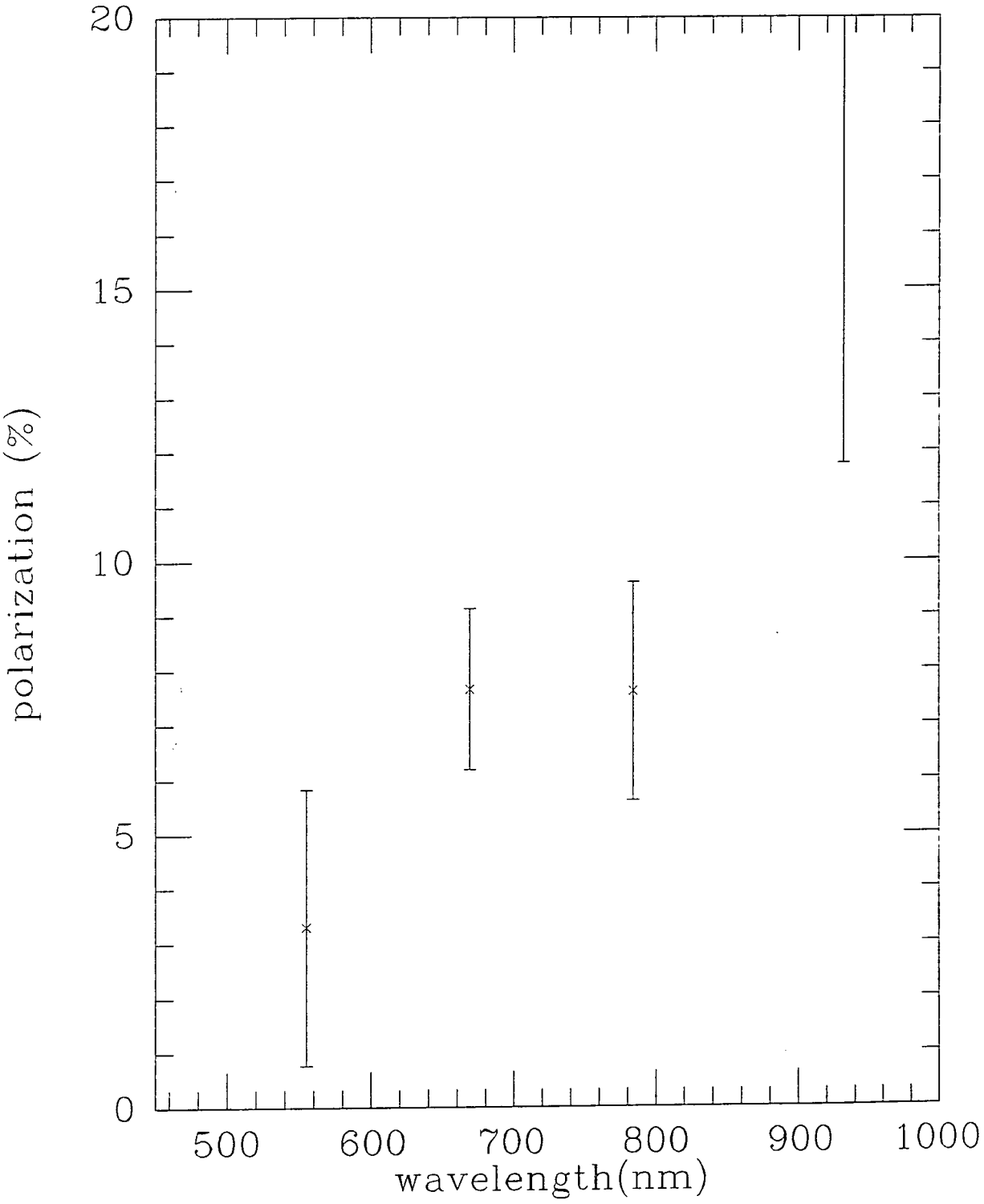
20
15
10
5
0
polarization (%)
500
600
700
800
900
1000
wavelength(nm)

Fig. 5.9

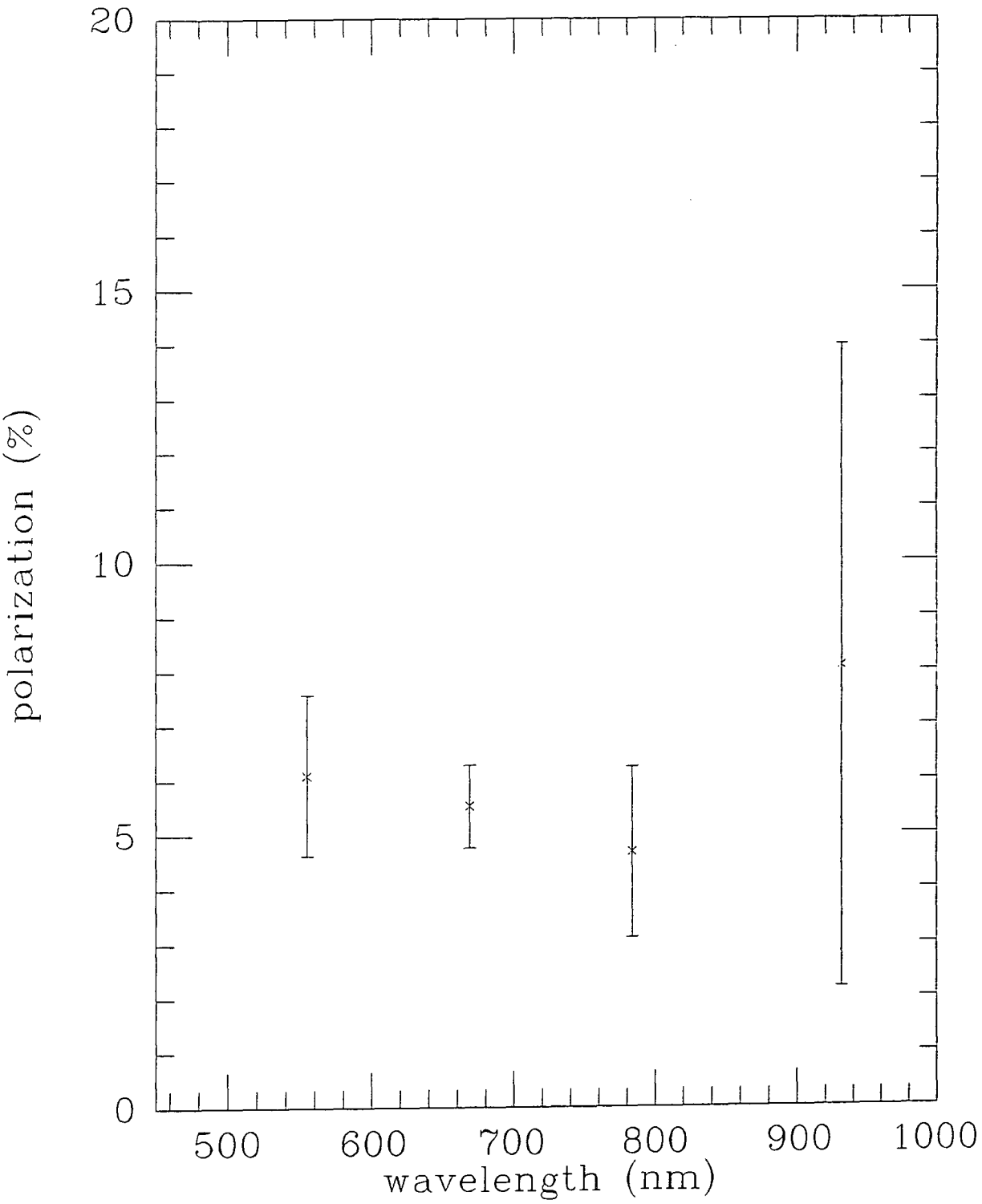
20
15
10
5
0
polarization (%)
500
600
700
800
900
1000
wavelength (nm)

Fig. 5.10

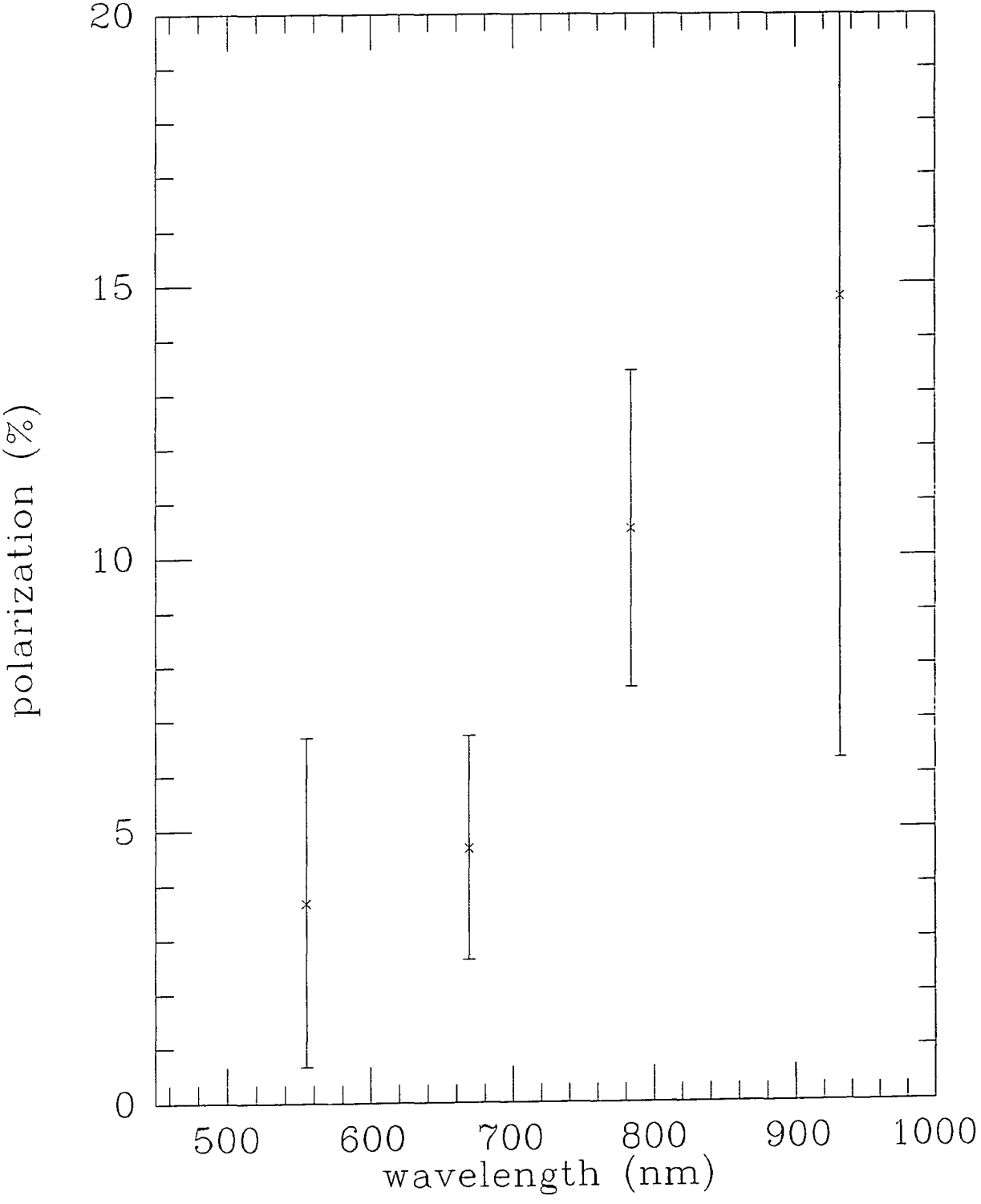
20
15
10
5
0
polarization (%)
500
600
700
800
900
1000
wavelength (nm)

Fig. 5.11

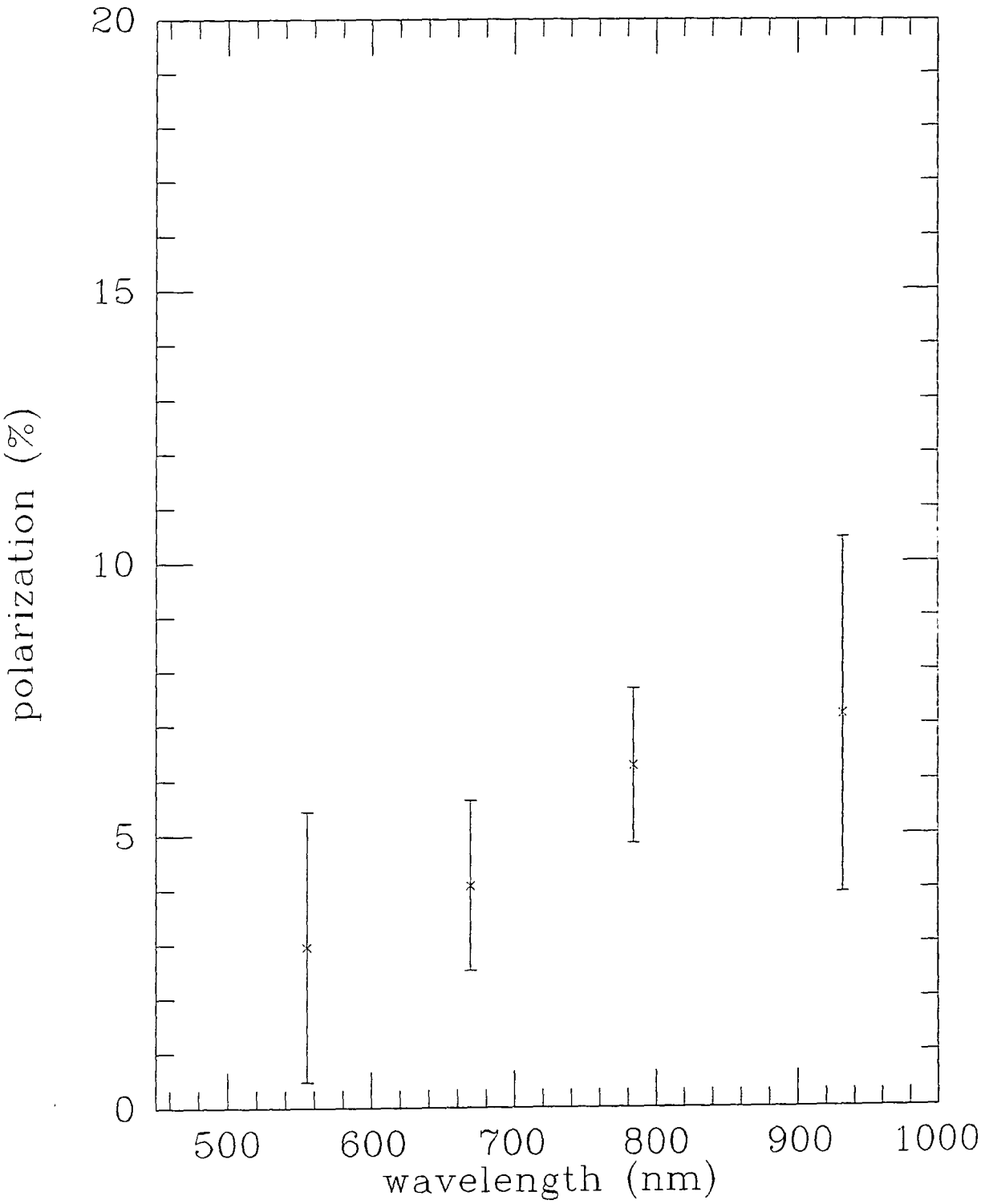
20
15
10
5
0
polarization (%)
500
600
700
800
900
1000
wavelength (nm)

Fig. 5.12

# CHAPTER SIX
# DISCUSSION OF THE DATA

## 1) INTRODUCTION

Reflection nebulae are formed by the scattering from dust of the light from a nearby star, e.g. the nebulosity surrounding the Pleiades. Such nebulosity generally shows a similar, but slightly bluer colour than that of the illuminating source, also the pattern of polarisation, caused by dust scattering around a single illuminating source, shows a centro-symmetric pattern, from which the actual position of the source can be located.

If we assume a reflection nebula model for the cone(IRN), by examining the circular pattern shown in the polarisation maps, then this would indicate an illuminating source at the position;

R.A. =-20 ± 5 arcsec

Dec.= 25 ± 5 arcsec

The co-ordinate system used here is such that the bright centre of the nebulosity is at the origin, and consistent with the approach adopted by Brosch and Greenberg (1985). Figure 6.1 shows the nebulosity and position A is where an illuminating source would be if it was a simple reflection nebula.

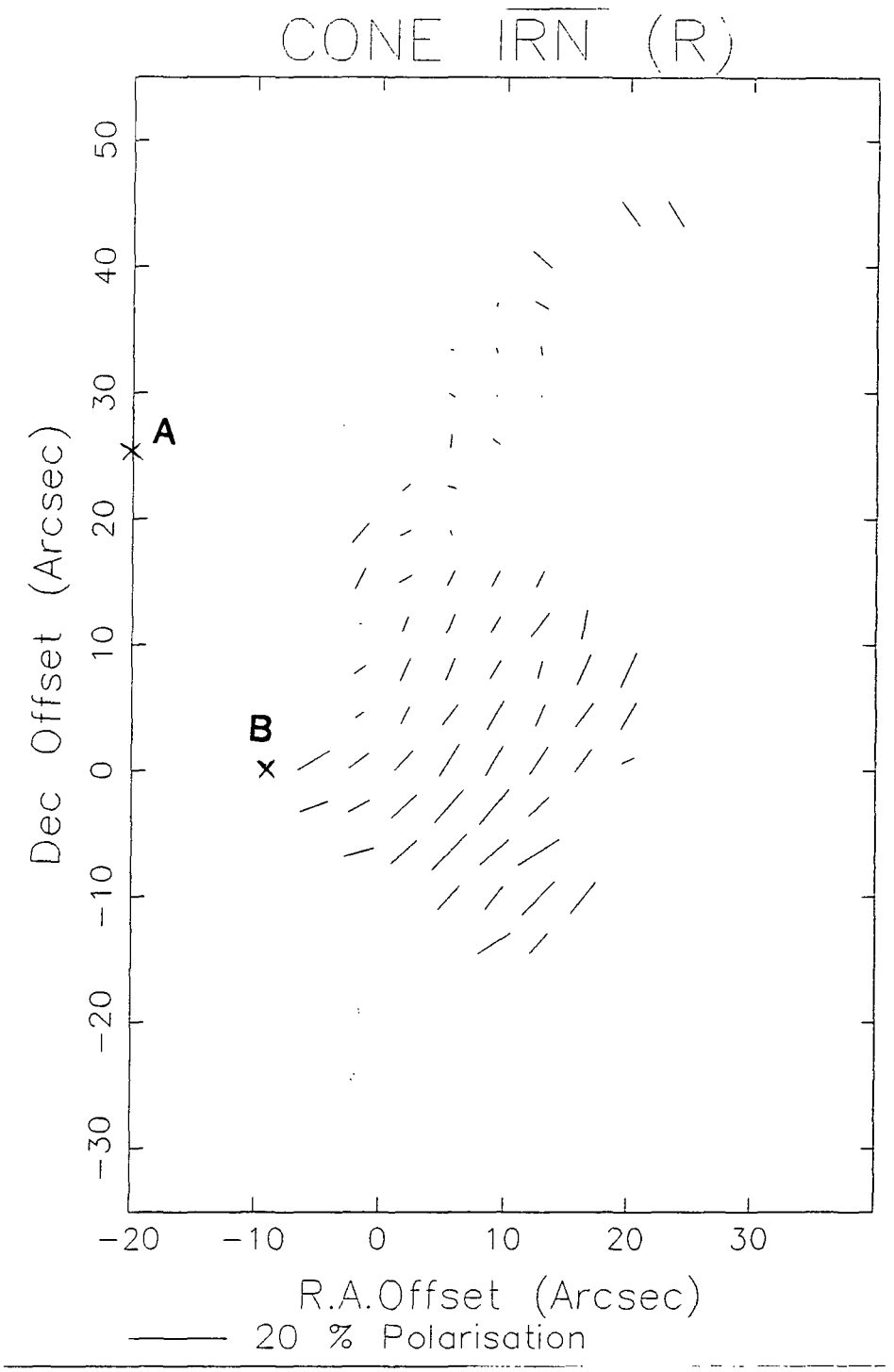


Fig. 6.1

**Locations of a possible source.**

Although stars are in the vicinity, there is no star present at the place where we would expect an illuminating source.

Using these co-ordinates, Allen's Infrared object would be located at approximately;

R.A.=-10 "

Dec.= 0 "

(See figure 6.1 position B.)

The polarisation pattern, however, does not indicate this object to be the illuminating source, which had been suggested in earlier models. So, if Allen's IR object is not the illuminating source, of a simple reflection nebula, then we must seek other possible alternatives. At the position where we would expect to find an illuminating source, nothing is visible on the Palomar prints, or in the CCD frames.

Since there is no optical source at the location suggested by the polarisation maps, an alternative would be to look for another Infrared source in the vicinity. Allen scanned the area on the Anglo-Australian telescope in 1986, and his findings were that the IR source GL989 was, in fact, the brightest object in the region. Although he found evidence of other IR emission in the vicinity, there was nothing at the position suggested by the polarisation pattern.

Allen made observations of the region in JHK images, and he found that at shorter wavelengths, the distribution of the nebulosity near to the IR source, looked very similar to that in the optical wavelengths. However, at longer wavelengths, the nebulosity was much more compact, and directed towards the north of the IR source.

So, it can be seen that perhaps that H and K images represent the central regions of the northern lobe of a cometary or bipolar nebula, which can only be seen at these wavelengths because of the high level of obscuration, and the polarisation maps are fairly consistent with this interpretation.

Photographs taken by Allen are shown overleaf, (figure 6.2), the first

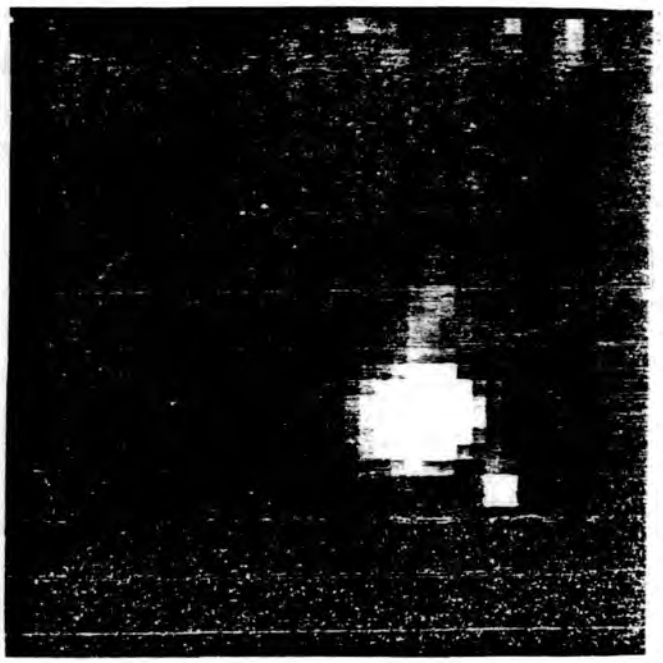

N

3.8 μm

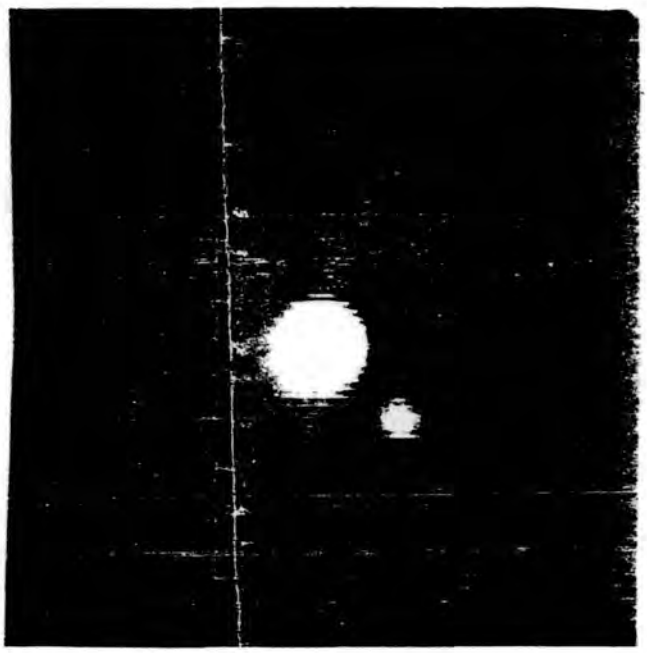

2.2 μm

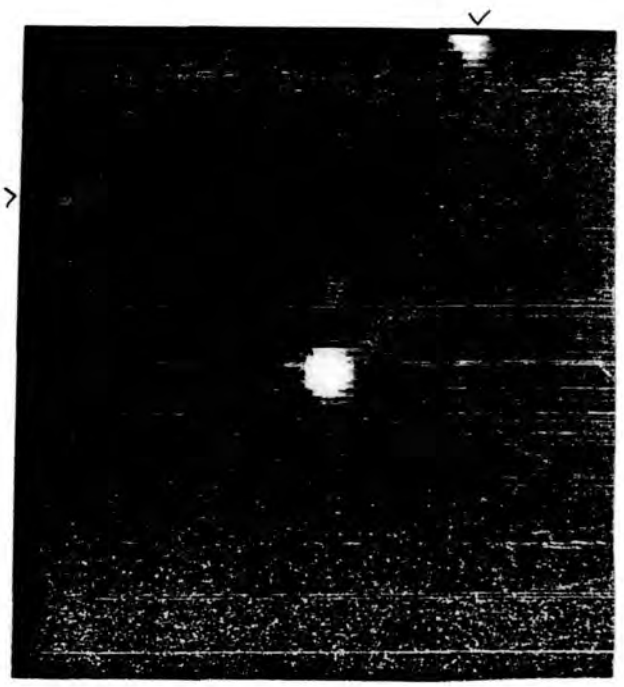

1.2 μm

Fig. 6.2

**Allen's JHK Images.**

picture is taken at 3.8 microns, with pixels of 1.8 arcsec square, and the frame is 72 arcsec square. The IR source is the brightest object, but there is also another infrared source lying to its south-west. There are other areas of infrared emission, but nothing near the position of the centre of polarisation, as shown on the polarisation maps. The second and third pictures show the source in a more centralised position, and the pixels have been interpolated to produce a more definitive outline of the source. The J map corresponds to 1.2 microns, and the K map corresponds to 2.2 microns. The J map shows the nebulosity extending to the upper right of the picture (north-east), whereas the K map shows the nebulosity extending in a more northerly direction. The third picture, corresponding to 1.2 microns, also shows two other stars which are in the periphery of the photographs.

This makes the polarisation maps much more interesting, for if it was a reflection nebula, then there must be a remarkable amount of extinction between the observer and the object itself. However, an alternative possibility is that the nebulosity does not arise from simple scattering and we must seek an alternative mechanism to explain the polarisation data. The IR source lies behind most of the dust, and is consequently heavily obscured, which is in agreement with the data.

The alternative mechanisms which can produce the observed polarisation are either grain alignment, or scattering. The grain alignment mechanism has been discussed earlier, in which the magnetic field aligns the elongated grains by the Davis-Greenstein mechanism. The aligned grains can then polarise the radiation by preferential absorption. In a scattering mechanism, however, the dust grains surround a central star, in which the geometry would be of an asymmetrical shape, such as in a disc or bipolar nebula.

## 2) SERKOWSKI'S RELATIONSHIP

The wavelength dependence of maximum interstellar linear polarisation was studied extensively by Serkowski et al (1969), for about 180 stars in the UBVR spectral regions. It was found that the normalised wavelength dependence of the interstellar linear polarisation (P), follows closely to a single empirical

curve, as outlined in chapter 2.

Serkowski's relationship between maximum interstellar linear polarisation and wavelength is given by;

$$P(\lambda)/P_m = \exp\{-1.15 \ln^2(\lambda_m/\lambda)\}$$

where $P_m$ is the maximum linear interstellar polarisation, and $\lambda_m$ is the wavelength at which it occurs.

The results showed that from most of the objects studied, the vast majority conformed to this generalised empirical pattern. However, following from this, in 1969, Serkowski and Robertson then began to investigate several regions of the sky which had produced values of the maximum wavelength which were either higher or lower than average. It was then suggested that the wavelength dependence of interstellar polarisation could be a good indicator of the variations in size of the associated interstellar dust grains.

If the values for the maximum wavelength were larger than average, it was thought that the polarisation is seen through a relatively dense dust cloud, with the size of the grains larger than average, and in some way connected to the observed larger value for maximum wavelength. It is now generally believed that the wavelength at which maximum polarisation occurs, $\lambda_{max}$ is proportional to the average size of the grains, and can produce both extinction and polarisation effects.

From his data, Serkowski established that the wavelength for maximum polarisation was generally about 545nm, with some regions such as Orion or Orphiuchus, having larger values, and hence indicating dense clouds with larger grain sizes. However, the Cygnus OB2 association had a smaller than average value for $\lambda_{max}$, at 410 nm (Savage and Mathis, 1979).

Serkowski also deduced that there was a relationship between the wavelength at which maximum polarisation occurs and the ratio of total to selective interstellar extinction, R;

$$R=5.5\ \lambda_{max.}$$

where $\lambda_{max}$ is the value of the wavelength at which maximum polarisation occurs, and is measured in microns.

If we use this equation, with a wavelength value of 0.545 microns, as this is the generally accepted average value, then this corresponds to a value of;

$$R=3$$

From the data obtained by studying the ConeIRN, it was then to be determined how the polarisation varied with wavelength for this particular object, and to compare with the pattern predicted by Serkowski's relationship.

The bright centre of the nebulosity, (0,0) using the coordinates as adopted in this study and explained earlier, was selected as requiring closer inspection. Figure 6.3 shows how the percentage polarisation varies at the associated wavelengths, and the curve corresponds to a possible Serkowski relationship, calculated for a maximum wavelength of 700nm, and a maximum polarisation value of 5 percent, as this presented an initial estimate to compare the response. The data obtained with the Z filter was not used for this calculation, as it seemed too inaccurate due to the errors involved.

Following this, a program was used to calculate the values of chi-squared as a function of wavelength, in order to obtain a more accurate value of the maximum polarisation ($P_{max}$), and the wavelength at which this occurs, $\lambda_{max.}$ Figure 6.4 shows the relationship between chi-squared and wavelength, and this gave the results that the maximum wavelength value was 750 nm, and the maximum polarisation value was 4.8 percent.

Using the data, further graphs were produced, figure 6.5 shows how the polarisation varies with wavelength at the position (0,0), in the nebulosity, and figure 6.6 shows the relationship between $P/P_{max}$ plotted against $\lambda_{max}/\lambda$

It can be seen that from our data, the value of $\lambda_{max}$ is 750nm., which is larger than Serkowski's average value of 545nm.

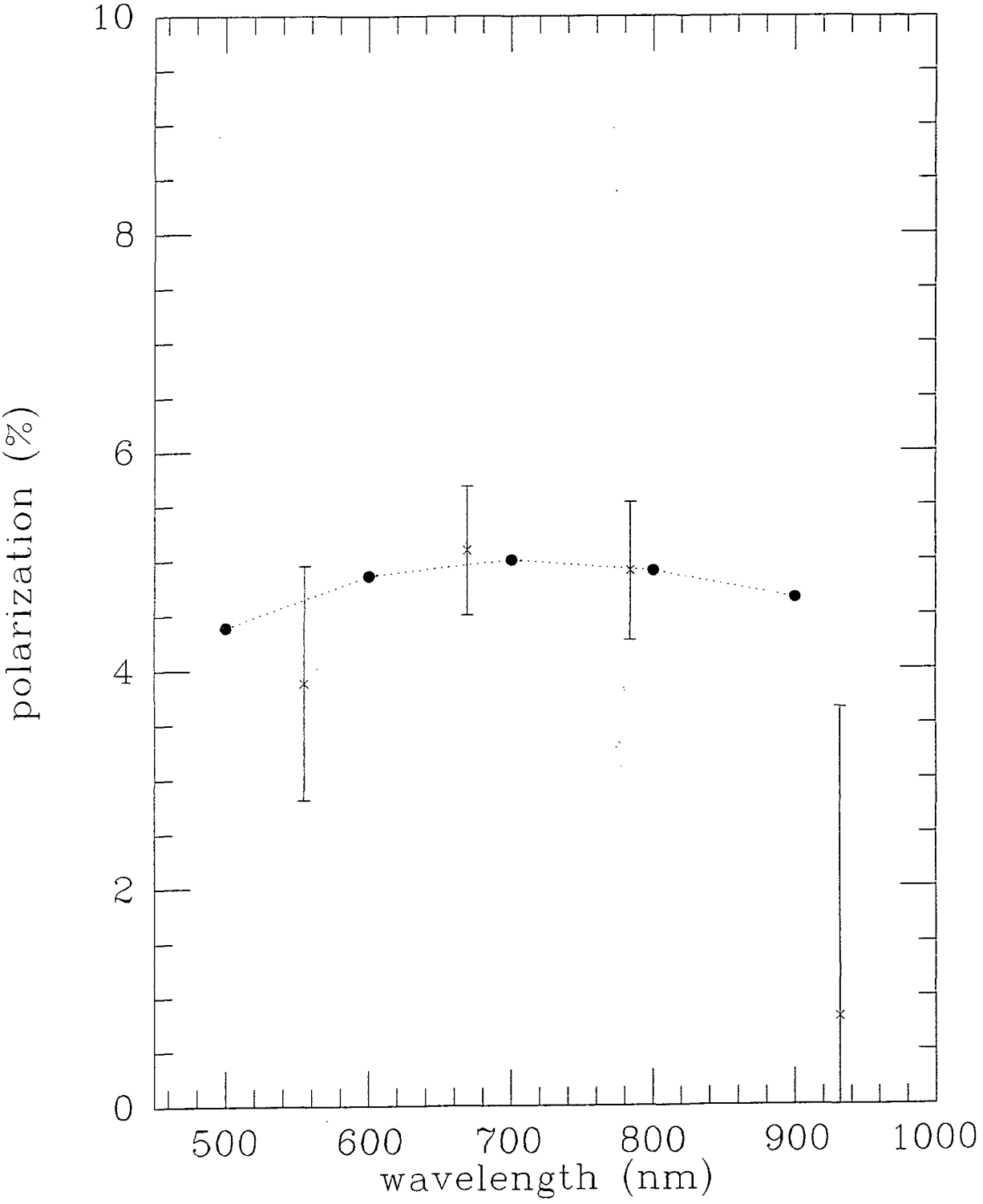
10
8
6
4
2
0
polarization (%)
500
600
700
800
900
1000
wavelength (nm)

Fig. 6.3

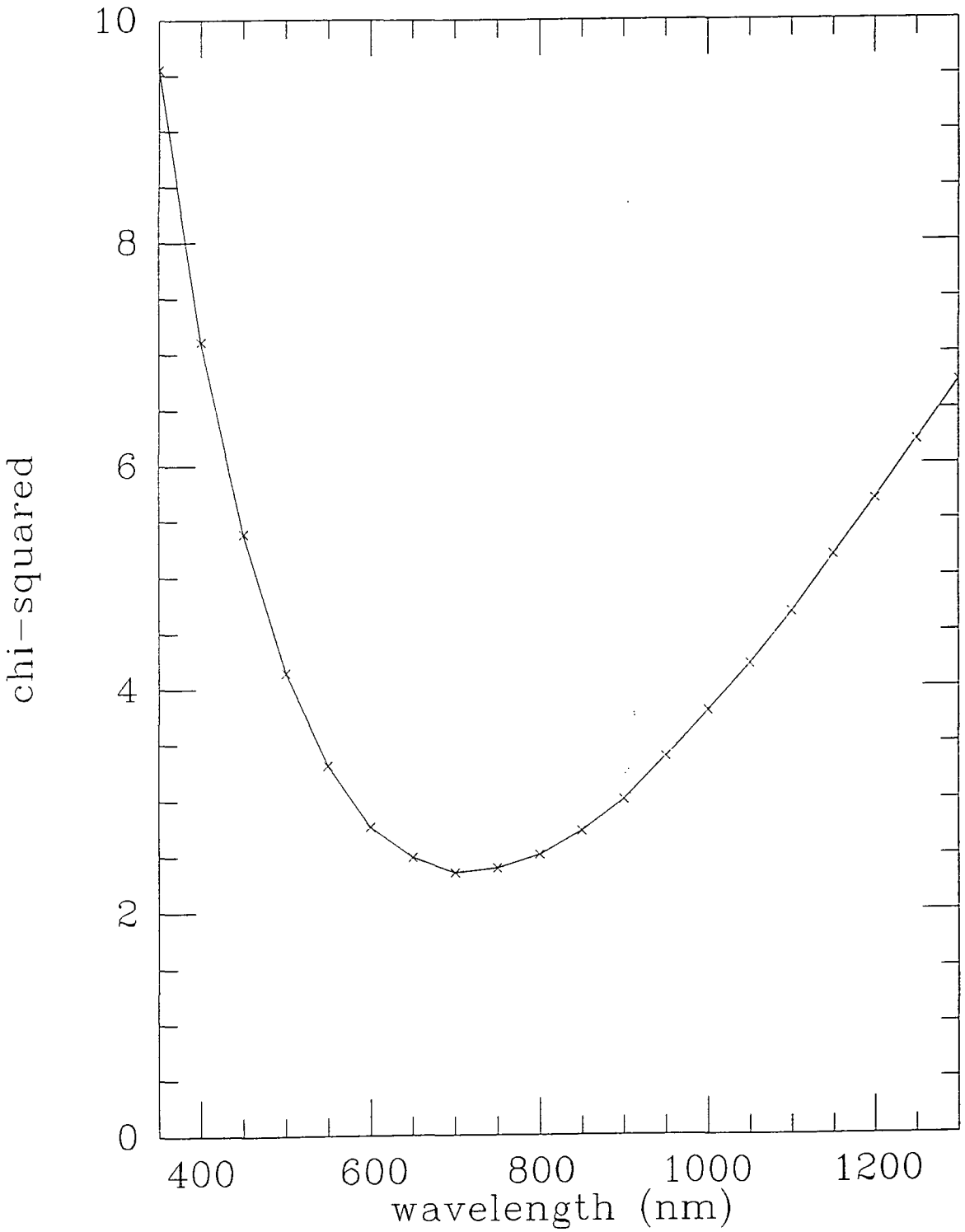


Fig. 6.4

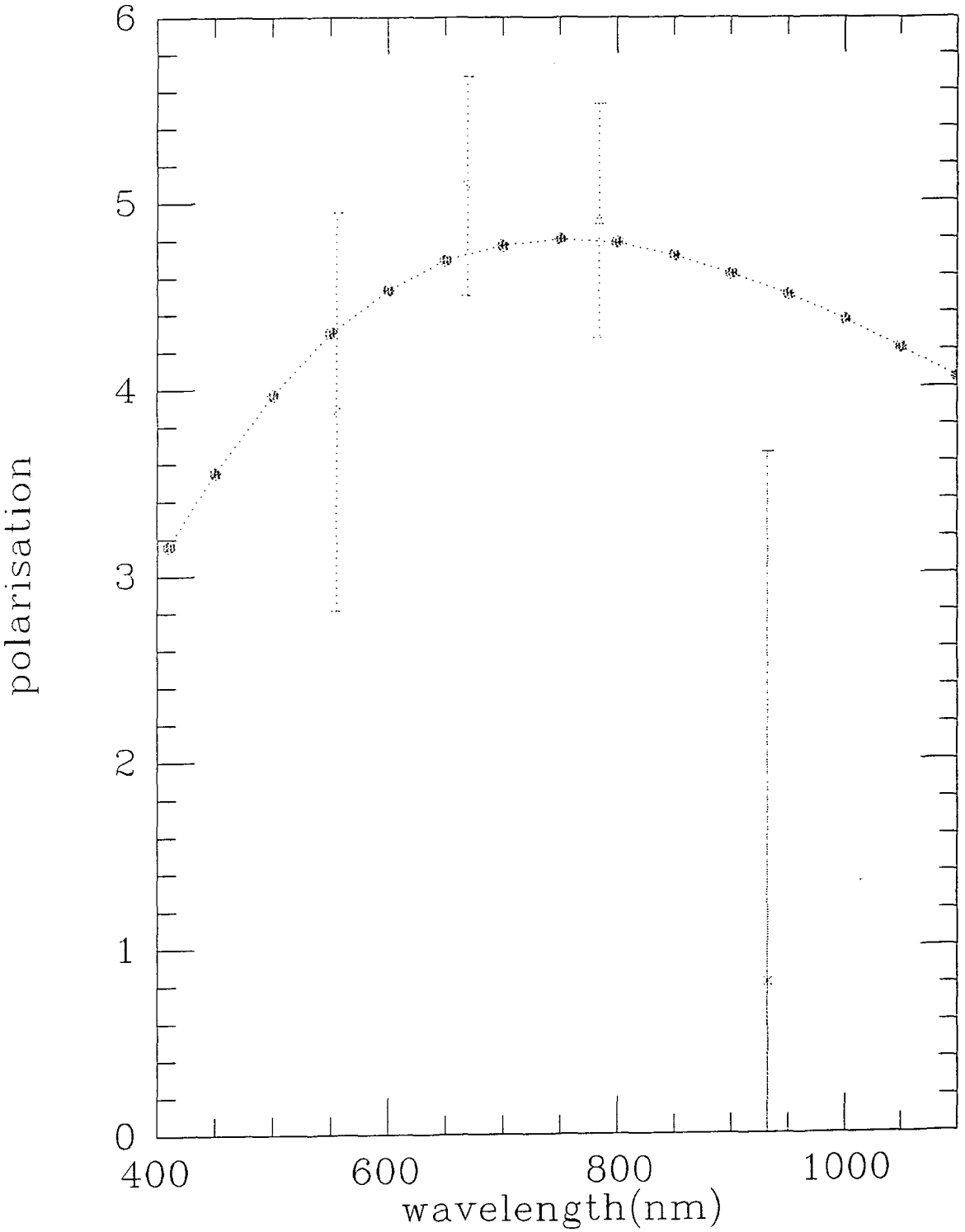


Fig. 6.5

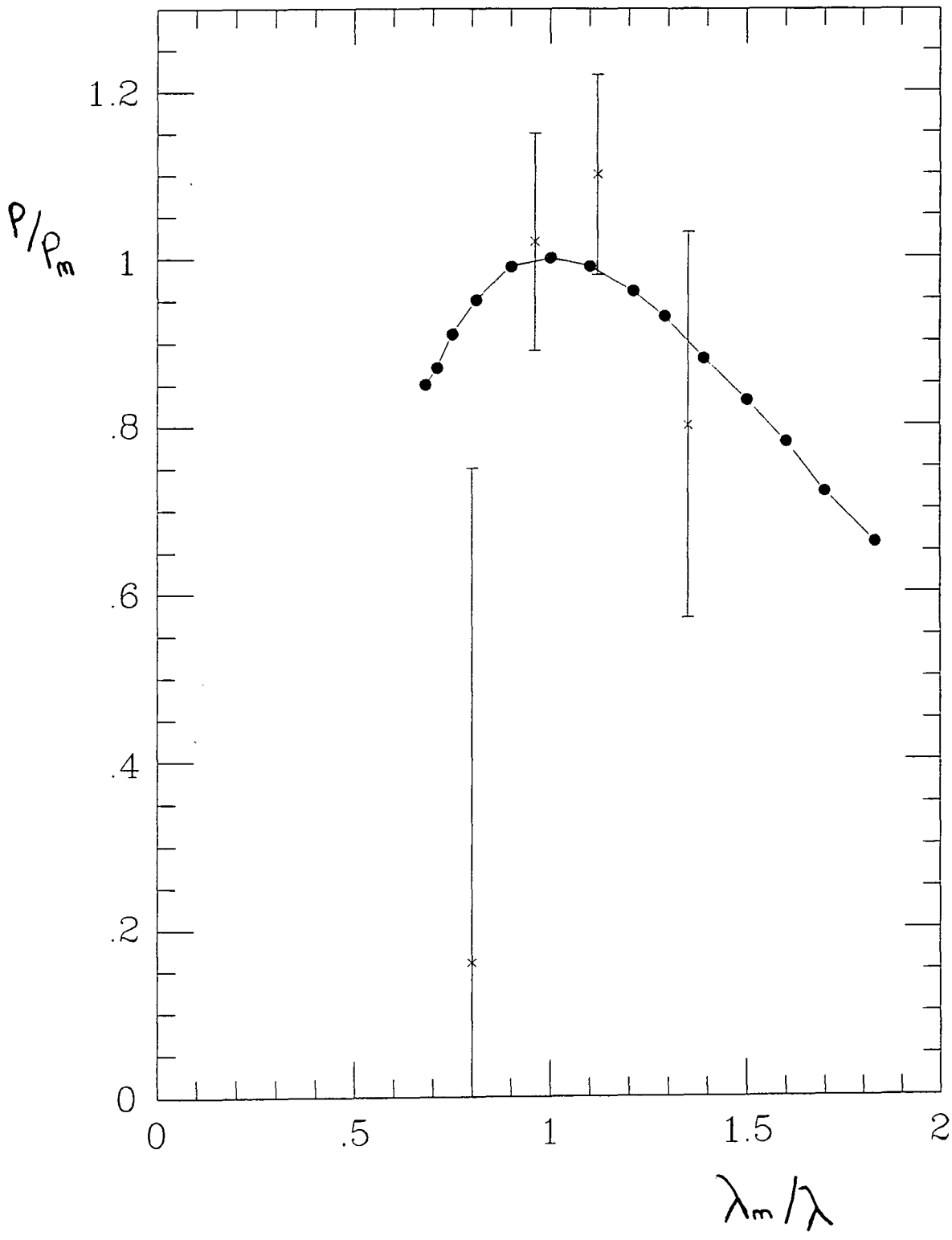


Fig. 6.6

From the equation;

$$R=5.5\ \lambda_{max}.$$

where R is the ratio of total to selective interstellar extinction,

$$R=5.5 \times 0.75 \text{ (microns)}$$

$$R=4.1 \pm 0.1$$

which is considerably higher than the average observed value of 3.0.

There is also a strong connection between this value of maximum wavelength and the grain size of the particles, as shown by Carrasco, Strom and Strom in 1973, with larger values of wavelength corresponding to dense dust clouds.

R.S. McMillan, (1977), found that unusually large values of the ratio of total to selective extinction (R), and the wavelengths of maximum interstellar linear polarisation were found in localised regions of dense interstellar clouds. For simplicity, he assumed that the grains were spherical, and from the relationship;

$$m = n\text{-}in'$$

where "m" is the complex refractive index of the grains, and in the interstellar medium, the value of "n" is approximately 1.33, which corresponds to low density dielectric materials; so m= 1.33-in'. McMillan then proceeded to relate the wavelength of maximum linear polarisation to the refractive index of the grains;

$$\lambda \propto \langle(n-1)a\rangle$$

in which the brackets denote the average values taken along the line of sight

to the observer, "a" is the mean grain radius, and "n" is the real part of the refractive index.

Since he assumed the value of "n" to be the same everywhere in the interstellar medium, (1.33), then $\lambda_{max}$ is directly proportional to the average grain size.

$$\lambda \propto \langle a \rangle$$

A further expression can be shown, which relates the enlarged grains in dense interstellar clouds to "normal" sized grains based upon the previous groundwork by Serkowski et al.

$$\frac{\lambda_m}{\lambda_{m,norm}} = \frac{\langle a \rangle}{\langle a \rangle_{norm}}$$

Since the observed value of $\lambda_{max}$ is generally taken as 0.55 microns, and with an assumed value of m=1.33, for the normal grains, then;

$$\langle a \rangle = 0.3 \text{ microns.}$$

$$\frac{\lambda_m}{0.55} = \frac{\langle a \rangle}{0.3}$$

From the data obtained from the ConeIRN, $\lambda_{max}$ was found to be 0.75 microns, which when substituted into the above equation gives a value for a, the mean grain size of the particles, to be;

$$\langle a \rangle = 0.41 \pm 0.1 \text{ microns.}$$

which, as predicted is larger than average for the interstellar medium.

McMillan found that in the extreme values of λ max, (HD147889 and W67), the evidence supported the concept of dielectric mantles growing on dielectric

grains, assuming Mie theory calculations for homogeneous and core-mantle spherical grains. However, this was for the special cases stated, whereas McMillan later went on to show that there was a possibility of long wavelength of maximum interstellar polarisation,and large values of R (ratio of total to selective extinction ) could be due to mantles of ice accreted onto the interstellar grains.

Whittet and Blades (1980), developed the relationship between the refractive index of the grains and $\lambda$ max, for whereas McMillan had assumed a constant value of 1.33 for both the cores and mantles of the grains, a value of n= 1.6 was introduced for silicates, which would have an affect on the grain size. However, if ice mantles condense onto silicate cores, then the assumption that n is a constant is invalid. The effect of reducing 'n' while keeping 'a' constant would be to reduce 'R' and $\lambda_{max}$.

Whittet, Bode and Evans, (1981), investigated how large values of R were connected to particle size. In particular, they studied HD29647 and found R to be at a value of 3.5 ± 0.1, which was higher than the accepted general value for the interstellar medium as being 3.1. They suggested from their findings that in this particular case, there were ice mantles on the grains, which was also supported by the observed anomalous ultra-violet extinction.

In the previous section, a value of R was calculated, and found to be R=4.1 ± 0.1 which is higher than the mean value for the interstellar medium. However, this was calculated using Serkowski's relationship of

$$R=5.5\ \lambda_{max}$$

Whittet and Van Breda (1980) found the need to modify this equation slightly, to take into account observational errors, and they showed that a corrected version was given by $R =(5.6 \pm 0.3)\ \lambda_{max}$, which is very close to the accepted value, within the experimental error. With this version, using the value for $\lambda$ max as 0.75 microns, gives a value of; $R= 5.6x0.75 = 4.2 \pm 0.2$

Grain growth leading to increases in values of R and $\lambda$ max may occur either by coagulation of grains due to increased collision rates in dense clouds

(Lefevre 1970), or by the condensation of material from gas on to the grain surfaces to become mantles (Greenberg 1968). Cohen (1977), however, deduced that the grain mantles must contain molecules including hydrogen, such as water ice, in the denser clouds.

## 3) FURTHER DISCUSSION

Heckert and Zeilik made extensive studies of protostellar infrared sources (1984), and produced polarisation maps at wavelengths of 2.2 microns, ( K waveband).

The maps were of high resolution and enabled them to determine the spatial dependence of polarisation in such sources, one of which was the coneIRN. The percentage polarisation had been determined previously at various wavelengths by Heckert and Zeilik in 1981;

TABLE 5

| waveband | | polarisation |
|---|---|---|
| J | 1.23 microns | 8.90 ± 3.7 % |
| H | 1.67 | 5.70 ± 0.8 % |
| K | 2.20 | 3.00 ± 0.2 % |
| L | 3.50 | 1.98 ± 0.3 % |

These results were taken with a 16" aperture over the peak of the maximum light intensity of the nebulosity, but their further observations which were with a 3.6" aperture, was specifically limited to the K waveband (2.2 microns). On the peak of the nebulosity, the new value was found to be 3.1 ± 0.2, which is consistent with the previous data. The percentage polarisation was given for specific areas of the nebulosity, confined to a square of sixteen arcsec with the brightness peak at the centre.

The polarisation map produced from the data, showed quite a different vector representation to the polarisation maps produced in the previous chapter. From their observations, they found within the coneIRN, there were two polarising mechanisms at work, both grain alignment and scattering. The evidence for grain scattering indicated that this was the primary mechanism involved, whereas the scattering was much less significant.

The latter mechanism was thought to be responsible for causing the polarisation at the regions north and south of the intensity peak. So in any attempts to interpret the configuration of the nebulosity, both mechanisms need to be taken into account.

The nature of the optical nebulosity near GL 989 IRS (Allen's Infrared source, was studied by Scarrott and Warren-Smith (1988). They found that the nebulosity (coneIRN) did not show the features of a typical reflection nebula, and suggested that the polarisation was due to dichroic extinction by aligned grains. The polarisation of a beam-like feature, apparently emanating from the infrared source was studied, and was believed to be a shaft of starlight escaping from the source and illuminating material along its path.

It has been found that some pre-main stage cometary and bipolar nebulae have produced polarisation patterns, which are not typical of simple reflection nebulae, illuminated by a central source. Some examples are; NGC 2261/ R. Mon ( Warren-Smith et al,1987; Scarrott et al, 1988) and also GM-29/PV Cephei (Gledhill et al. 1987), HH46/47 ( Scarrott et al. 1988 ).

In these examples, an interesting feature has arisen, where the orientation of the polarisation vectors appear to be aligned with the bright rims of the lobes of the nebulae.

NGC 2261 is of particular interest, and figure 6.7 shows a polarisation map of the nebulosity, as observed by Scarrott et al., NGC 2261 (Hubbles variable nebula), appears to be excited and illuminated by the nearby star R.Mon., and it is a good example of a cometary nebula associated with the process of star formation. The nebulosity is much more complicated than just a simple reflection nebula, and the polarisation has undergone marked changes in the past decade, particularly in the orientation of the polarisation disc.

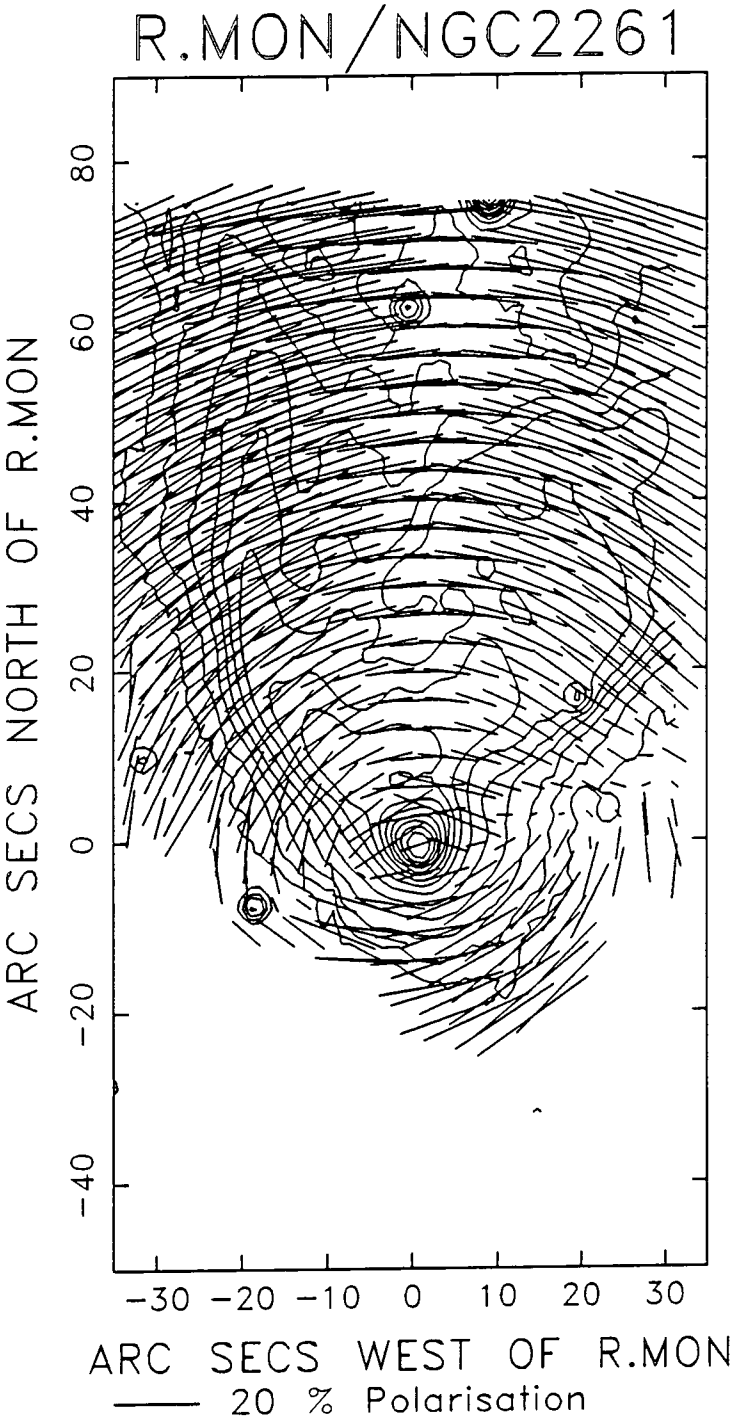
R.MON/NGC2261
ARC SECS NORTH OF R.MON
80
60
40
20
0
-20
-40
-30 -20 -10 0 10 20 30
ARC SECS WEST OF R.MON
20 % Polarisation

Fig. 6.7

It was suggested that the radiation has been scattered, within the circumstellar disc, from a central source which emits the polarised light. It is also believed that subsidiary effects occur, perhaps due to extinction by magnetically aligned grains in the larger disc surrounding R. Mon.

The optical nebulosity is the visible counterpart of a much larger complex, that includes a bipolar outflow collimated by an extensive gas and dust ring surrounding R. Mon. The system is tilted to the line of sight of the observer, with the northern outflow directed towards us, and corresponding to part of the optical nebulosity, whereas the southern component of the nebulosity is totally obscured.

The nebulosity associated with RE50, (Reipurth and Bally, 1986) is another possible cometary nebula development, which, in this case has an Infrared source near to the nebulosity, but it also has a shaft of starlight illuminating dark cloud material.

So, in any attempts to explain the mechanisms involved with the polarisation of the Cone IRN, these examples can illustrate the various different processes and geometries involved. In developing a model, however, it is necessary to review the data with respect to the possible mechanisms involved.

A model which has been discussed earlier is the Elsasser and Staude model, which is relevant to the modelling of the ConeIRN. In this model, there is a central stellar source embedded symmetrically in a disc like configuration of dust and gas, which is further surrounded by an extended tenuous cloud. The optical thickness of the disc is supposed to be large in directions along the equator, while optically thin at the polar regions of the disc, with some unpolarised direct light escaping from the central star. This would then give rise to an increase of the net polarisation with increasing optical depth.

Elsasser and Staude applied this model to the Becklin - Neugebauer object, and assumed a central source radiating as a black body with a temperature of 600 K. The circumstellar material was thought to consist of silicate and ice particles, and the opacities and scattering cross-sections of the grains were computed with Mie theory.

The variable star PV Cephei is of particular interest at this point in the discussion. Over the past few decades, the nebulosity associated with PV Cephei has shown marked changes in structure. In the Poss plates, taken in 1952, the nebulosity was seen to be linear in shape, rather like a streak, and it appeared to emanate from PV Cephei. However, by 1976, the streak seemed to have developed into a sort of fan-shaped nebulosity, having the star at the apex. Cohen et al. (1981) noted the changes in the luminosity of the nebula, as the star changed in brightness of several magnitudes within a few months. The former streak shape seemed now to be a part of the eastern edge of the fan. Recently, however, the nebulosity has became more bipolar in shape, and situated within an asymmetric distribution of matter about a magnetic field. (Gledhill et al, 1986)

A model was suggested for the PV Cephei system which involved a T Tauri-type star, (PV Cephei), formed within a small dense globule and surrounded by a circumstellar Torus containing gas and dust. This torus allowed a conical beam of light from PV Cephei to illuminate the material ejected from the star, which was experiencing variable mass loss, and resulting in the observed cometary nebula. The axis of the system is tilted out of the plane of the sky, so that the fan of nebulosity is closer to us than the star. The bar-like structure which is located a few arcsec north of the star corresponds to the inner edge of the torus, which is experiencing shock excitation due to the strong stellar wind which is coming from PV Cephei. Levreault (1984) found a bipolar molecular outflow (CO) centred on PV Cephei, with the northern part of the outflow blue-shifted, which confirmed the tilt of the axis as suggested by Cohen previously (1981). Scarrott et al. (1986) found that there was a faint "counterfan" to the south of PV Cephei which corresponded to the red-shifted outflow of the Levreault model. This was the first indication of the bipolarity of the system.

The polarisation maps which were produced for PV Cephei and the surrounding nebulosity exhibited an unusual pattern of linear polarisation, with little of the centro-symetric arrangement of vectors normally associated with reflection nebulae. The polarisation pattern is largely due to the polarising

effects of non-spherical dust grains which are aligned by the local magnetic field. Polarisation by Scattering mechanisms are of less significance. The asymmetric material which surrounds PV Cephei partly obscures background light from the faintly luminous surrounding cloud, and part of this material overlies the extreme eastern edge of the nebula, where it produces strong reddening and the associated polarisation effects.

By comparing the Cone IRN with the suggested model for the PV Cephei system, we can interpret some of the observations. We could suggest that the Cone IRN is in the very process of evolving from pre main sequence into a cometary or bipolar nebula. In this case, Allen's Infrared object (GL989) would be the protostar, which is gradually creating cavities in the dark cloud material. The small fan-shaped nebulosity which we have been referring to as the Cone IRN is the first visible trace of one of the cavity walls. If this is the case, then we can make further parallells, and suggest that, in time, the nebulosity will develop into a more obvious shape and structure. The light detected in the nebula possibly originates in the protostar, and will be multiply scattered and heavily extinguished in the rather dense surrounding material. As a consequence of this, then the magnetically aligned dust grains in the dense medium can then produce polarisation, by means of dichroic extinction, and this would take precedence over any polarisation produced in the scattering process.

In the model for PV Cephei proposed by Gledhill et al. (1987), then during the pre-stellar collapse, the magnetic field in the surrounding dark cloud material was drawn inwards towards the protostar and then produced a toroidal configuration within the circumstellar disk around the central object. So if we apply this model to the cone IRN, then it appears that the radially orientated field aligns the dust grains, but as the obscuration surrounding the object is so high, we can not, as yet, detect a circumstellar disk in any of the optical data.

## 4) CONCLUSION.

The polarisation data seems to indicate that the small fan-shaped nebulosity, known as the ConeIRN, is not just a simple reflection nebula illuminated by a protostar. In fact, it is proposed that the nebula is the beginnings of the edge of a cavity which is being created by outflows from Allen's Infrared object (GL989), and the polarisation occurs due to the extinction by magnetically aligned grains which heavily obscure the region. These grains are located in a circular envelope around the actual source itself, close to the proposed cavity. The polarisation is perpendicular to the major axis of the cavity. Furthermore, it is believed to be in the early stages of developing into a cometary nebula, having many similarities with other pre-main stage nebulosities.

The shape and structure of the nebula is therefore expected to exhibit marked changes in development over the next few decades.

# REFERENCES.


Adams, M.T., Strom, K.M., and Strom, S.E., 1983 *Astrophysical journal,* **53** 893

Appenzeller, I., 1967 *Publ.astr.Soc.pacific* **79** 136

Allen, D.A., 1972. *Astrophysical journal,* **172** L52 - 58

Baade, W., 1944 *Astrophysical journal* **100** 137

Bastien, P., & Menard, F., 1988 *Astrophysical journal* **326** 324

Blitz, L., 1978 *NASA TM* 79708

Breger, M., 1972 *Astrophysical journal* **171** 539

Brosch, N., and Mayo Greenberg, J., (1985) private communication.

Carrasco, L., Strom, S.E., Strom, K.M., 1973 *Astrophysical journal* **182** 95

Cederblad,S., 1946 *Medd.lunds.astr.obs.* **2** 119

Cohen, J.G., 1977 *Astrophysical journal,* **214** 86

Cohen, M., Kuhi, L.V., Harlan, E.A., Spinrad, H., 1981 *Astrophysical journal* **245** 920

Coyne, G.V., Gehrels, T., Serkowski, K., 1974 *Astrophysical journal* **79** 581

Coyne, G.V., and Wickramasinghe, N.C. 1969 *Astrophysical journal* **74** 1179

Crutcher, R.M., Hartkopft, W.I., and Giguere, P.T., 1978 *Astrophysical journal,* **226** 839

Davis, L., and Greenstein, J.L., 1951 *Astrophysical journal* **114** 206

Dorschner, J., Gurtler, J., 1965 *Astr.Nach.* **289** 57

Draper, P.W., 1988 PhD thesis, University of Durham.

Eiroa, C., Elsasser, H., and Lahulla, J.F. 1979 *Astron. Astrophys.*

Elsasser, H., and Staude, H.J., 1978 *Astron. Astrophysics* **70** L3-6

Elvius, A., Hall, J.S., 1966 *Lowell Obs.Bull.* 6 **135** 257

Gehrels, T., 1960 *Astrophysical journal* **65** 470

Genzel, R., and Downes, D. 1977 *Astron.Astrophys supp.* **30** 145

Gledhill, T.M., Warren-Smith, R.F., and Scarrott, S.M., 1987 *Mon.Not.R.astr.Soc.* **229** 643

Gledhill, T.M. and Scarrott, S.M., 1989 *Mon.Not.R.ast.Soc.* **236** 139

Gold, T., 1952 *Mon.Not.R.ast.Soc.* **112** 215

Greenberg, J.M., 1960 *Astrophysical journal* **132** 672

Greenberg, J.M., 1968 "Nebulae and Interstellar matter" University of Chicago press.
Greenberg, J.M., and Hong, S.S., 1975 *"The dusty universe",* N. Watson Academic publications.
Hall, J.S., and Hiltner, W.A., 1949 *Science* **109** 165
Harvey, P.M., Campbell, M.F., Hoffmann W.F., 1977 *Astrophysical journal* **215** 151
Heckert, P.A., and Zeilik, M., 1981 *Astrophysical journal* **86** 1076
Heckert, P.A., and Zeilik, M., 1984 *Astrophysical journal* **89** 1379
Herbig, G., 1962 *Astrophysical journal* **135** 736
Hiltner, W.A., 1949 *Science* **109** 165
Hollenbach, D. and Salpeter, E.E., 1979 *Astrophysical journal* **163** 155
Iben, I., and Talbot, R.J., 1966 *Astrophysical journal* **144** 968
Johnson, P. E., 1982 *Nature* **295** 371
Keenan, P.C., 1936 *Astrophysical journal* **84** 600
LeFevre, J., 1970 *Astron.Astrophys* **5** 37
Levreault, R.M. 1984 *Astrophysical journal* **277** 634
Lucas, R., LeSequeren, A.M., Kazes, I., Encrenez, P.J., 1978 *Astron.Astrophysics* **66** 155
McMillan, R.S., 1977 *Astrophysical journal* **216** L41
Meyer, W.F., 1920 *Lick Obs.Bull* **10** 68
Mie, G. 1908 *Ann. physik* **25** 377
Morton, D.C., 1974 *Astrophysical journal* **193** L35
Notni, P., 1985 *Astr.Nach.* **306** 265
Ohman, Y., 1939 *Mon.Not.R.astr.Soc.,* **99** 624
Perkins, H.G., King, D.J., Scarrott, S.M., 1981a *Mon.Not.R.astr.Soc.* **196** 403
Pickering, E.C., 1873 *Amer.Acad.Arts.Sci.* **9** 1
Racine, R., 1968 *Astrophysical journal* **73** 233
Reipurth, B., & Bally, J., 1986 *Nature* **320** 336
Rickard, L.J., Palmer, P., Buhl, D., and Zuckerman, B., 1977 *Astrophysical journal* **213** 654
Salpeter E.E., 1977 *An.Rev.Ast.Astrophysics.* **15** 267
Savage, B.D. and Mathis, J.S., 1979 *Astron.Astrophysics* **17** 73
Scarrott, S.M., 1988 *Mon.Not.R.astr.Soc.*, **231** 1055

Scarrott, S.M., Draper P.W., and Warren-Smith, R.F., 1989 *Mon.Not.R.astr.Soc.* **237** 621-634.

Scarrott, S.M., Warren-Smith, R.F., Pallister W.S., Axon,D.J., Bingham.R.G., 1983 *Mon.Not. R. astr.Soc.* **204** 1163-1177

Scarrott, S.M., and Warren-Smith R.F., 1988 *Mon.Not.R.ast.Soc.* **232** 725

Schmidt, E.G., 1972 *Astrophysical journal* **176** L69

Schmidt, E.G., 1974 *Mon.Not.R.ast.Soc.* **169** 97

Schmidt. G.D., Angel, J.R.P., Beaver E.A., 1978 *Astrophysical journal* **219** 477

Schwartz, P.R., 1985 *Astrophysical journal* **292** p231

Schwartz, P.R., Thronson, H.A., Odenwald, S.F., Glaccum, W., Loewenstein, R.F. and Wolf, G. 1985 *Astrophysical journal* **292** 231-237.

Serkowski, K., 1962 *"Advances in Astronomy and Astrophysics"* Academic press

Serkowski, K., and Robertson, J.W., 1969 *Astrophysical journal* **158** 441

Serkowski, K., 1974 *IAU Collaq* **23** 135

Serkowski, K., Mathewson, D.S., and Ford, V.L. 1975 *Astrophysical journal.* **196** 261-290.

Simon, T., Simon, M., Joyce, R.R., 1979 *Astrophysical journal* **230** 127

Spitzer, L. and Tukey, J.W. 1951 *Astrophysical journal* **114** 187

Struve, O. 1936 *Astrophysical journal* **84** 219

Taylor, K.N.R., Scarrott, S.M., 1980 *Mon.Not.R.astr.Soc.* **193** 321

Thompson, R.I. and Tokunaga, A.T. 1978 *Astrophysical journal* **226** 119

Van de Hulst, H.C., 1981 "Light scattering by small particles" Dover Publications Inc.

Van den Bergh, S. 1966 *Astrophysical journal* **71** 990

Walker, M.F., 1956 *Astrophysical journal supp.* **2** 365

Walker, M.F., 1972 *Astrophysical journal* **175** 89

Walsh.J.R., 1980 *Astrophysics and Space Science.* ***69*** 227-254

Warner, J.W., Strom, S.E., and Strom, K.M., 1977 *Astrophysical journal.* **213** 427.

Warren-Smith, R.F., 1979 Ph.D. thesis, University of Durham

Warren-Smith, R.F., 1983 *Mon.Not.R.ast.Soc.*, **205** 349

Warren-Smith, R.F., Draper, P.W., & Scarrott, S.M., 1987 *Astrophysical journal* **315** 500

Wells, D.C., Greisen, E.W., and Harten, R.H. 1981 *Astron.Astrophys.Supp.* **44** 363

Whittet, D.C.B., 1984 *Mon.Not.R.astr.Soc.* **210** 479-487

Whittet, D.C.B., Blades J.C., 1980 *Mon.Not.R.astr.Soc.* **191.** 309-319.

Whittet, D.C.B., Van Breda, I.G., 1980 *Mon.Not.R.ast.Soc.* **192** 467

Whittet, D.C.B., Bode, M.F., Evans, A., and Butchart. 1981 *Mon.Not.R.ast.Soc* **186** 81P.

Wickramasinghe, N.C., 1973 "Light scattering functions for small particles with applications in Astronomy" Adam Hilger, London.

Witt, A.N., and Schild, R.S., 1986 *Astrophysical journal* **62** 839-852.

Wright, J.S., and MacKay, C.D., 1981 *Proc.Soc. Phot.Inst.Eng.* **290** 160

Zuckerman, B., Morris, M., Palmer, P., and Turner, B.E., 1972 *Astrophysical journal (letters)* **173** L125

## ACKNOWLEDGEMENTS.

This is the part where I can now say 'thank you' to all the people who have helped me in the past few years, and express my gratitude. I would first of all like to thank my supervisor, Dr. S.M. Scarrott, for his patience, support and encouragement throughout this time. Secondly, I would like to thank the others in the Durham Polarimetry group, whose friendship and advice have been appreciated; Chris Rolfe, Dominic Semple, Neasa Foley, Tim Gledhill and Peter Draper. I must also thank Alan Lotts and Nick "read it in the manual" Eaton for their help with the computing. I am also very grateful to Pauline Russell for help with the diagrams and reprographics.